

# Supplementary Material for “Direct photolysis of carbonyl compounds dissolved in cloud and fog droplets”

*Scott A. Epstein\*, Enrico Tapavicza, Filipp Furche, and Sergey A. Nizkorodov*

Department of Chemistry, University of California, Irvine

1102 Natural Sciences 2, Irvine, CA 92697-2025

\*Correspondence to: Scott A. Epstein (scott.a.epstein@gmail.com)

## Table of Contents

<b>1. Hydration of Dicarboxyls .....</b>	<b>4</b>
<b>2. Extinction Coefficients of Aqueous D-Glyceraldehyde and Dihydroxyacetone .....</b>	<b>5</b>
<b>3. FTIR Spectrum of Gaseous Photolysis Products.....</b>	<b>6</b>
<b>4. Monitoring the Photolysis of Glyceraldehyde Using a UV-Vis Spectrometer .....</b>	<b>8</b>
<b>5. Monitoring the Photolysis of D-Glyceraldehyde with ESI-MS .....</b>	<b>9</b>
<b>6. Reproductions of Figure 6 Under Different Atmospheric Conditions .....</b>	<b>11</b>
<b>7. Literature Values for <math>\epsilon_{\max}</math> and <math>\lambda_{\max}</math> .....</b>	<b>17</b>
<b>8. Evaluation of the Aqueous Photolysis Rate Constant Parameterization .....</b>	<b>18</b>
<b>9. Comparing Aqueous Photolysis with Aqueous Oxidation by OH at a pH of 6 .....</b>	<b>19</b>
<b>10. Predicted kOH as a Function of Molecular Structure .....</b>	<b>20</b>
<b>11. Computational Analysis of Additional Atmospherically Relevant Compounds.....</b>	<b>22</b>

12.	<b>Molecular Dynamics Simulation Molar Extinction Plots</b> .....	23
13.	<b>Tabular Extinction Coefficients of Glyceraldehyde and Dihydroxyacetone</b> .....	29
14.	<b>Expected Chemical Mechanism of Glyceraldehyde Photolysis</b> .....	33
15.	<b>Comparison of Aqueous Photolysis and Aqueous Oxidation by OH for 4-hydroxy-3-methyl-but-2-enal, 3,6-oxoheptanoic acid, ketolimonaldehyde, and ketonorlimonic acid</b> ...	35
16.	<b>Parameters Used to Construct Figure 3</b> .....	36
17.	<b>Structure of Molecules in Figure 3</b> .....	37
18.	<b>Parameters Used to Construct Figures 4 and 5</b> .....	38
19.	<b>Parameters Used to Construct Figures 2, 6, and S9-S13</b> .....	39
20.	<b>References</b> .....	51

## Table of Figures

Figure S1:	Molar extinction coefficients for D-glyceraldehyde and dihydroxyacetone.....	5
Figure S2:	D-glyceraldehyde absorbance as a function of concentration of the free form .....	6
Figure S3:	Apparatus used to capture and analyze the gases evolved from photolysis of glyceraldehyde .....	7
Figure S4:	FTIR spectrum of the products of aqueous D-glyceraldehyde photolysis at 25°C.....	8
Figure S5:	Absorption of glyceraldehyde photolysis solution as a function of time at 25°C.....	8
Figure S6:	Results of a calibration experiment relating the concentration of glyceraldehyde and the peak intensity of the derivatized glyceraldehyde adduct.. .....	9
Figure S7:	Semi-quantitative measurements of glyceraldehyde concentration as a function of photolysis time at 25°C for three separate experiments.....	10
Figure S8:	ESI-MS difference spectrum showing the formation of products and the disappearance of reactants from a typical glyceraldehyde photolysis experiment.....	11
Figure S9:	Reproduction of Figure 6 in the manuscript with a solar zenith angle of 0°. LWC = 0.5 g m <sup>-3</sup> , T = 25°C, pH = 2, and C <sub>OH</sub> = 10 <sup>-13</sup> M.....	12
Figure S10:	Reproduction of Figure 6 in the manuscript with C <sub>OH</sub> = 2.5 x 10 <sup>-14</sup> M. Solar zenith angle is 20°, LWC = 0.5 g m <sup>-3</sup> , T = 25°C, and pH = 2.....	13
Figure S11:	Reproduction of Figure 6 in the manuscript with LWC = 0.05 g m <sup>-3</sup> . Solar zenith angle is 20°, T = 25°C, pH = 2, and C <sub>OH</sub> = 10 <sup>-13</sup> M. ....	14
Figure S12:	Reproduction of Figure 6 in the manuscript with pH = 6. Solar zenith angle is 20°, LWC = 0.5 g m <sup>-3</sup> , T = 25°C, and C <sub>OH</sub> = 10 <sup>-13</sup> M.....	15
Figure S13:	Uncertainty estimates in the parameters Q and Z arising from calculations of model parameters .....	16
Figure S14:	Comparison of Q-values calculated with published extinction coefficients as a function of wavelength and Q-values calculated with our λ <sub>max</sub> and ε <sub>max</sub> parameterization .....	19
Figure 15:	Comparison of aqueous photolysis at a solar zenith angle of 20° and aqueous oxidation by OH at a typical daytime concentration of 10 <sup>-13</sup> M and a pH of 6. ....	20
Figure S16:	Aqueous rate constants for oxidation by OH as a function of carbon number. ....	21
Figure S17:	Aqueous rate constants for oxidation by OH as a function of hydrogen number ....	22

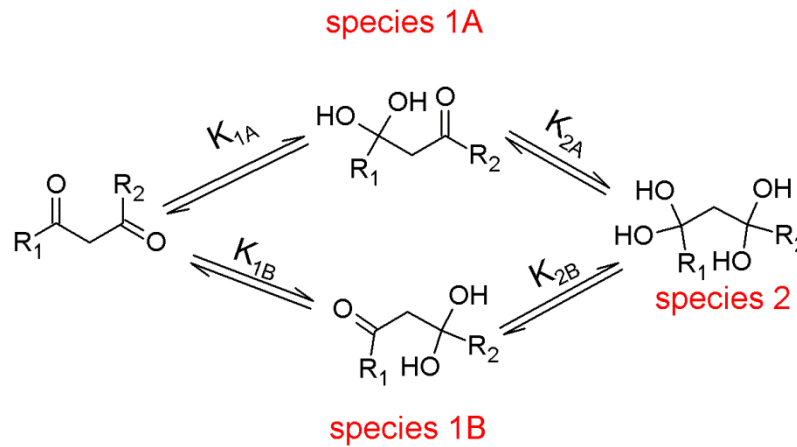
Figure S18: Calculated MD extinction coefficients for gaseous and aqueous levulinic acid [4-oxopentanoic acid].	23
Figure S19: Calculated MD extinction coefficients for gaseous and aqueous pyruvaldehyde [2-oxopropanal].	24
Figure S20: Calculated MD extinction coefficients for gaseous and aqueous 3-oxobutanal.	24
Figure S21: Calculated MD extinction coefficients for gaseous and aqueous 2,3-butanedione [biacetyl].	25
Figure S22: Calculated MD extinction coefficients for gaseous and aqueous pyruvic acid [2-oxopropanoic acid].	25
Figure S23: Calculated MD extinction coefficients for gaseous and aqueous glyceraldehyde [2,3-dihydroxypropanal].	26
Figure S24: Calculated MD extinction coefficients for gaseous and aqueous 4-hydroxy-3-methyl-but-2-enal.	26
Figure S25: Calculated MD extinction coefficients for gaseous and aqueous 3,6-oxoheptanoic acid.	27
Figure S26: Calculated MD extinction coefficients for gaseous and aqueous ketolimononaldehyde.	27
Figure S27: Calculated MD extinction coefficients for gaseous and aqueous ketonorlimonic acid.	28
Figure S28: Chemical Mechanism of Glyceraldehyde Photolysis	34
Figure S29: Comparison of aqueous photolysis at a solar zenith angle of 20° and aqueous oxidation by OH at a typical daytime concentration of 10 <sup>-13</sup> M and a pH of 2.	35

## Supplementary Material Tables

Table S1: $\epsilon_{\max}$ and $\lambda_{\max}$ values used to determine aqueous photolysis rates for Figures 6, and S9-S12	17
Table S2: Structures corresponding to the molecules listed in Table S1	18
Table S3: Calculated $\epsilon_{\max}$ and $\lambda_{\max}$ values for compounds found in d-limonene and isoprene SOA	22
Table S4: Measured extinction coefficients of glyceraldehyde	29
Table S5: Measured extinction coefficients of dihydroxyacetone	32
Table S6: Computational and experimental parameters used to model the SOA relevant compounds plotted in Figure 3.	36
Table S7: Molecular structures of SOA relevant compounds investigated in Figure 3	37
Table S8: References and parameters used to generate Figures 4 and 5	38
Table S9: Henry's Law constants used to construct Figures 2, 6, and S9-13	39
Table S10: Hydration equilibrium constants and acid-dissociation constants used to construct Figures 2, 6, and S9-13	43
Table S11: Aqueous and gas-phase OH oxidation rate constants used to construct Figures 2, 6, and S9-13	47

## 1. Hydration of Dicarboxyls

This section describes our approach to account for hydration equilibria in dicarbonyl compounds. Consider an unhydrated and unsymmetrical dicarbonyl with carbonyl groups identified by the letters “A” and “B” (Scheme S1). In the aqueous phase, hydration can reversibly replace carbonyl “A” with a gem-diol group forming species 1A (equilibrium constant for the hydration process,  $K_{\text{hyd}} = K_{1A}$ ) and/or carbonyl “B” with a gem-diol group forming species 1B ( $K_{\text{hyd}} = K_{1B}$ ). A certain fraction of the mixture may be double hydrated, with both carbonyl groups converted in the gem-diol form. The corresponding equilibrium constants,  $K_{2A}$  and  $K_{2B}$  are identified in scheme S1.



Scheme S1: Hydration of a generic dicarbonyl

The molar fraction that is unhydrated,  $\alpha_{\text{un}}$ , fully-hydrated,  $\alpha_{\text{fh}}$ , and partially-hydrated,  $\alpha_{\text{ph}}$ , can be derived from the equilibrium equations (all activity coefficients are set to unity):

$$\alpha_{\text{uh}} = (1 + K_{1A} + K_{1B} + K_{1B}K_{2B})^{-1} \quad (1)$$

$$\alpha_{\text{fh}} = ((K_{1B}K_{2B})^{-1} + K_{2A}^{-1} + K_{2B}^{-1} + 1)^{-1} \quad (2)$$

$$\alpha_{\text{ph}} = 1 - (\alpha_{\text{uh}} + \alpha_{\text{fh}}) \quad (3)$$

Because the gem-diol form is lacking the  $\pi^* \leftarrow n$  transition associated with the carbonyl group, it is appropriate to assume that the rates of photolysis of the singly hydrated dicarbonyl species are approximately one-half of the rate of photolysis of the unhydrated form, resulting in the following expression for Z:

$$Z = \frac{\frac{dn_{\text{hv}}^{\text{gas}}}{dt}}{\frac{dn_{\text{hv}}^{\text{aq}}}{dt}} \geq \frac{\alpha_{\text{uh}} + 0.5\alpha_{\text{ph}}}{(R \cdot T \cdot LWC_v \cdot k_H)} \quad (4)$$

## 2. Extinction Coefficients of Aqueous D-Glyceraldehyde and Dihydroxyacetone

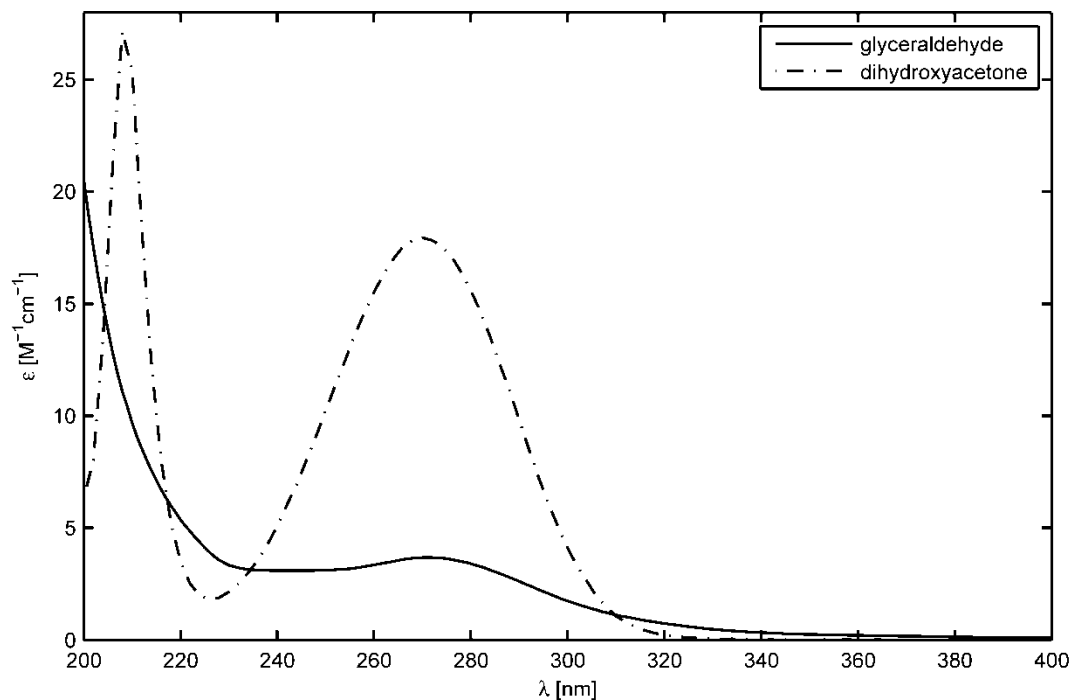


Figure S1: Molar extinction coefficients for D-glyceraldehyde (solid curve) and dihydroxyacetone (dashed curve) at 25°C calculated by dividing the absorbance by the total concentration (free + hydrated form). Note the only free form absorbs at 270 nm.

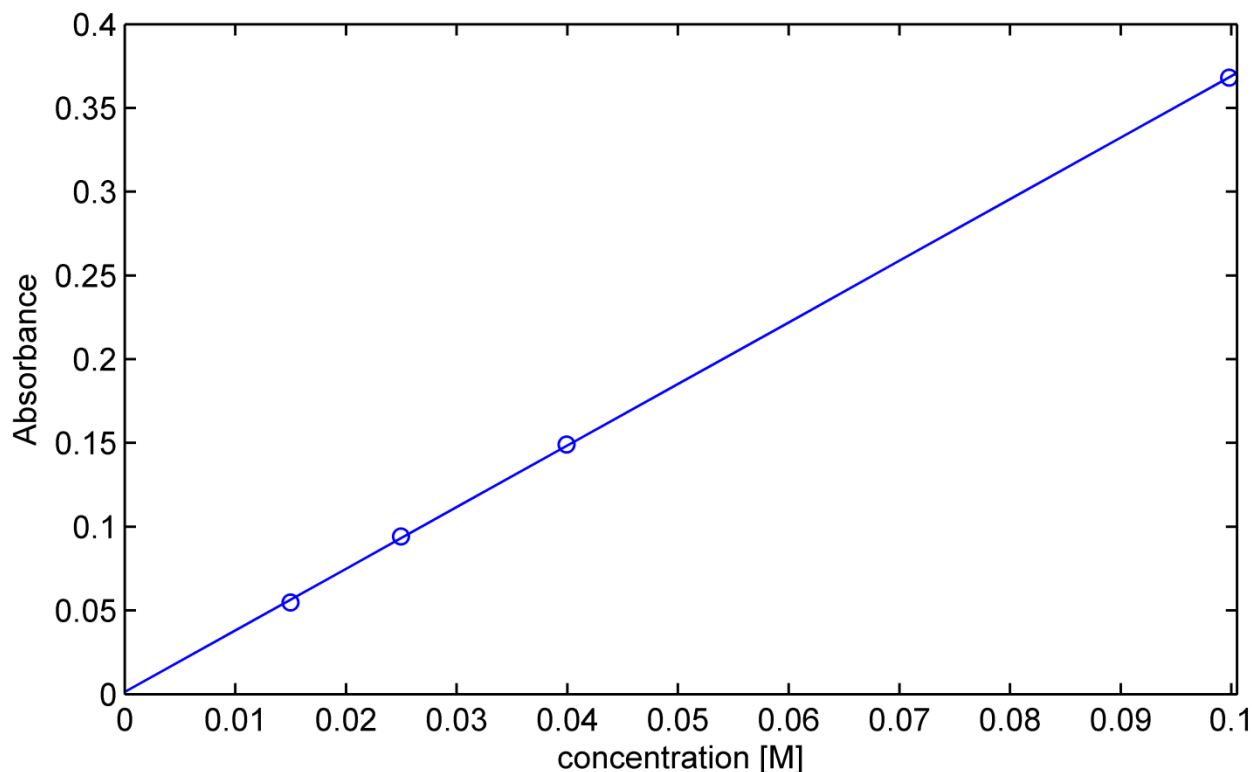


Figure S2: D-glyceraldehyde absorbance at 271 nm as a function of total concentration (free + hydrated form).

Figure S1 shows the molar extinction coefficients for D-glyceraldehyde (solid curve) and dihydroxyacetone (dashed curve) at 25°C that were measured in this work. A Beer-Lambert plot of the measurements is shown in Figure S2. Tabulated extinction coefficients are presented in Table S4 and S5. Both glyceraldehyde and dihydroxyacetone exhibit a well defined  $\pi^* \leftarrow n$  band that overlaps the solar flux. The  $\pi^* \leftarrow n$  band in D-glyceraldehyde is considerably lower in intensity compared to that in dihydroxyacetone because the former is much more prone to hydration than the latter. Specifically, the observed extinction coefficient (the one plotted in Figure S1) is reduced relative to the extinction coefficient of the unhydrated form of the molecule:

$$\epsilon_{observed} = \frac{\epsilon_{unhydrated}}{1 + K_{hyd}} \quad (5)$$

For D-glyceraldehyde, this reduction is substantial as  $1 + K_{hyd} = 18.3$  (Glushonok et al., 1986), much smaller than the corresponding value for dihydroxyacetone,  $1 + K_{hyd} = 1.77$  (Glushonok et al., 2003; Davis, 1973).

### 3. FTIR Spectrum of Gaseous Photolysis Products

Photolysis of aqueous D-Glyceraldehyde produced gas bubbles that formed on the walls of the photolysis cell. The gases produced during photolysis of aqueous D-Glyceraldehyde at 25°C were captured and analyzed with a Fourier Transform Infrared (FTIR) spectrometer (Mattson Galaxy Series 5000). A diagram illustrating the FTIR cell is presented in Figure S3.

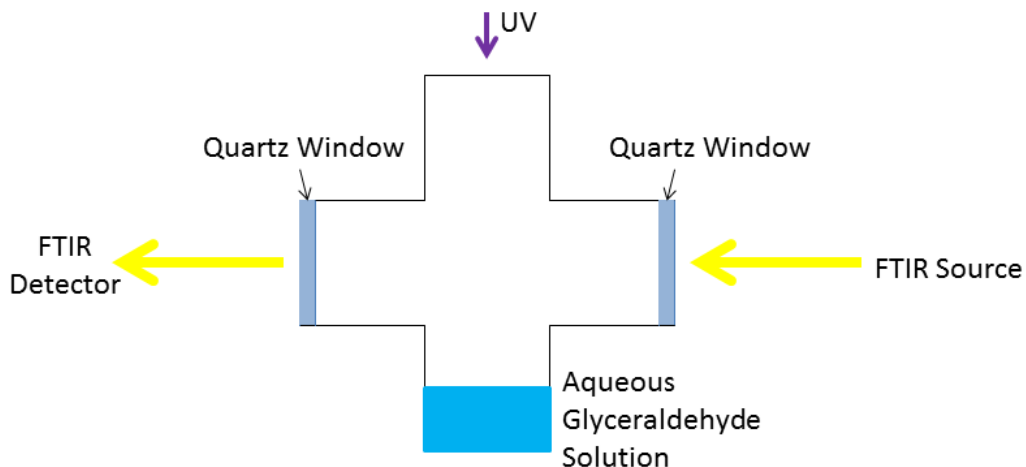


Figure S3: Apparatus used to capture and analyze the gases evolved from photolysis of glyceraldehyde

The FTIR spectrum shown in Figure S4 indicates the presence of carbon monoxide. Carbon monoxide is an expected product of the direct photolysis of D-Glyceraldehyde (see below). We have not attempted to quantify the yield of this product. The FTIR spectrum also indicates the presence of carbon dioxide, a potential product of secondary photolysis. However, we cannot conclude that the carbon dioxide evolved from the photolysis due to the potential presence of CO<sub>2</sub> from the ambient air.

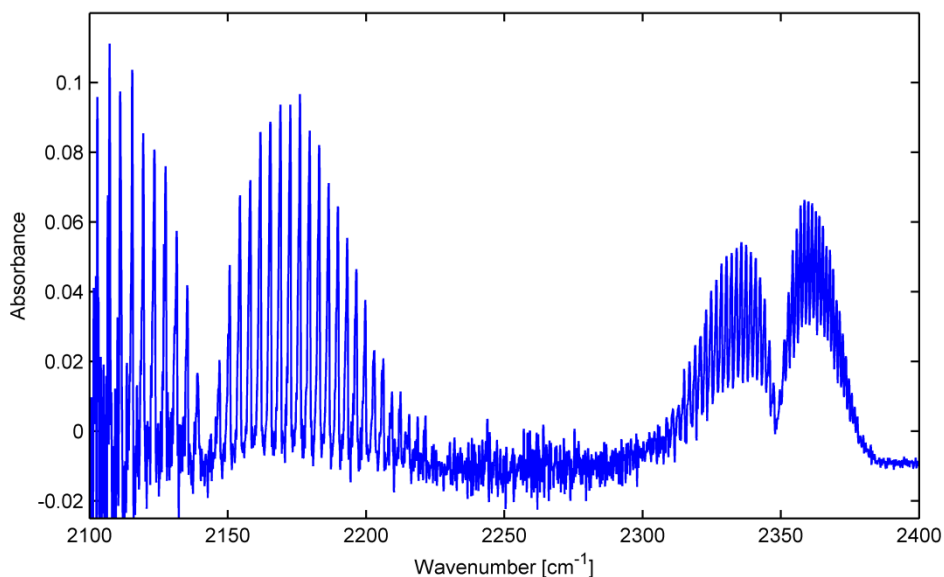


Figure S4: FTIR spectrum of the products of aqueous D-glyceraldehyde photolysis at 25°C. The band centered at 2143  $\text{cm}^{-1}$  belongs to carbon monoxide, and the band centered at 2349  $\text{cm}^{-1}$  is the asymmetric stretch of  $\text{CO}_2$ .

#### 4. Monitoring the Photolysis of Glyceraldehyde Using a UV-Vis Spectrometer

We took UV-Vis spectra measurements during photolysis of 0.1 M aqueous glyceraldehyde solutions at various photolysis times. Figure S5 shows how the absorption of an aqueous glyceraldehyde solution changes when exposed to UV light with a 40 nm bandwidth centered at 300 nm at 25°C.

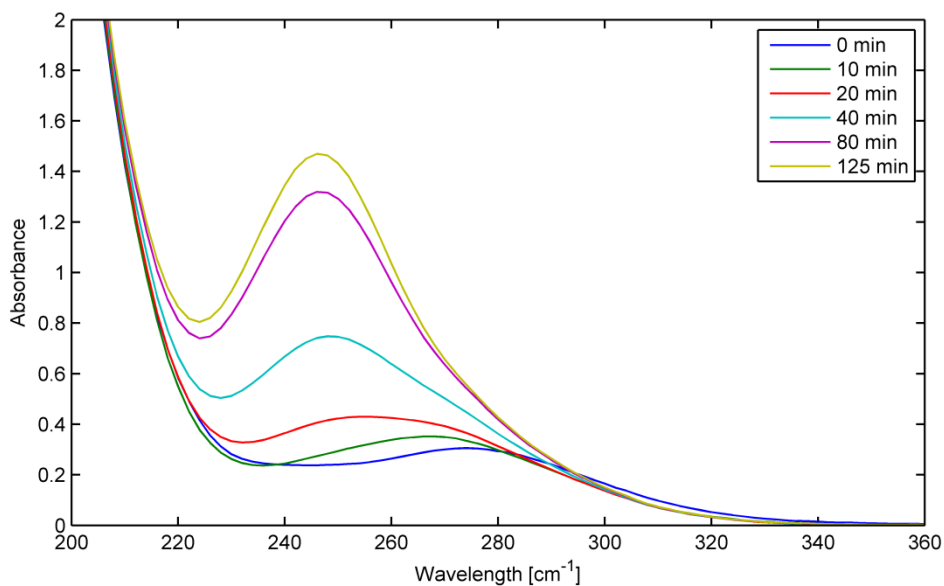


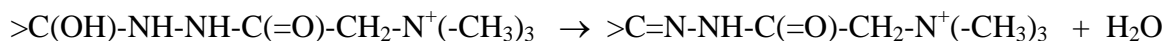
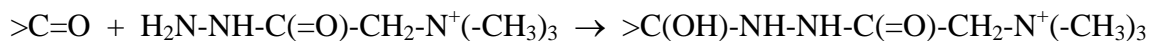
Figure S5: Absorption of glyceraldehyde photolysis solution as a function of time at 25°C



Upon photolysis, the  $\pi^* \leftarrow n$  band undergoes a simultaneous hypsochromic and hyperchromic shift. We believe that the band growing at 250 nm belongs to a minor but strongly absorbing photolysis product (which we could not identify because of its small concentration).

## 5. Monitoring the Photolysis of D-Glyceraldehyde with ESI-MS

We calibrated the ESI-MS technique for determining glyceraldehyde solution concentration before each photolysis experiment. Several glyceraldehyde solutions of varying concentrations were derivatized with Girard Reagent T (GT) and analyzed with an ESI-MS instrument. Reaction of carbonyls with the GT ion ( $C_5H_{14}N_3O^+$ ) leads to permanently positively charged adducts according to the reactions below. The first step generates a carbinolamine ion with  $m/z$  that is 132.1131 higher than the mass of the parent carbonyl molecule. Subsequent dehydration of the carbinolamine intermediate results in the final hydrazone product and an overall shift of 113.0953 between the  $m/z$  of the observed ion and exact mass. Only hydrozone products were observed in our experiments.



Tetraethylammonium chloride was added to the GT solution to act as an internal ESI-MS standard (it does not react with carbonyls and is expected to have a similar ionization efficiency to GT and GT+carbonyl adducts). Figure S6 illustrates a typical calibration curve determined with this method. The calibration is approximately linear.

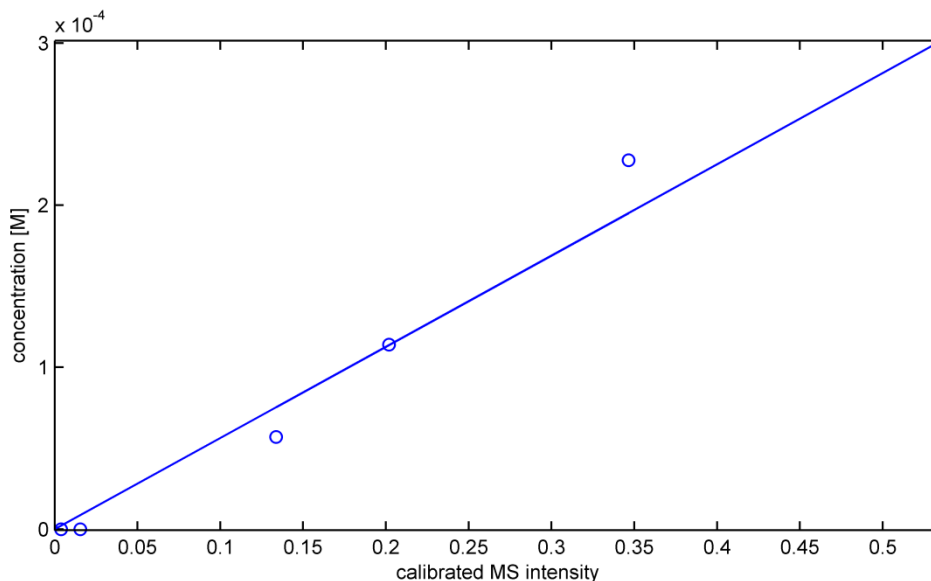


Figure S6: Results of a calibration experiment relating the concentration of glyceraldehyde and the peak intensity of the derivatized glyceraldehyde hydrazone adduct. The ion abundance of the glyceraldehyde-GT peak was normalized by that of the tetraethylammonium internal standard peak.

During a photolysis experiment, 100  $\mu\text{L}$  aliquots of the glyceraldehyde solution were withdrawn from the photolyzed solution periodically and added to 25 mL of a solution containing 0.9 mM GT and 0.05 mM tetraethylammonium chloride. This mixture was allowed to react overnight, forming the GT-glyceraldehyde adduct. The normalized glyceraldehyde-GT adduct peak abundance is shown in Figure S7 as a function of the photolysis time.

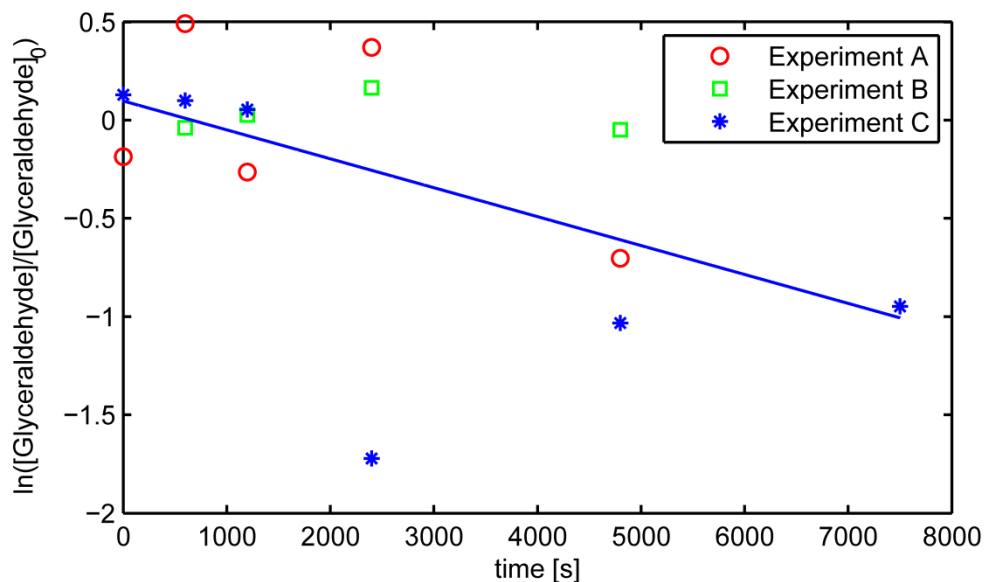


Figure S7: Semi-quantitative measurements of glyceraldehyde concentration as a function of photolysis time at 25°C for three separate experiments.

The observed scatter is due to the difficulties in quantifying the derivatized product with ESI-MS (and possibly due to incomplete GT+carbonyl reactions). The experiment indicated with the blue asterisks has an extreme outlier at 2300 s. However this outlier does not significantly affect the slope of the fitted line as it is close to the center of the x-axis. The slope of the fitted line, along with the known flux from the UV lamp obtained from actinometer measurements, were used to approximate the quantum yield of photolysis.

ESI-MS measurements were also used to identify potential photolysis products. Figure S8 shows an ESI-MS difference spectrum. Positive peak heights indicate that a product was formed while negative peak heights indicate the consumption of a reactant.

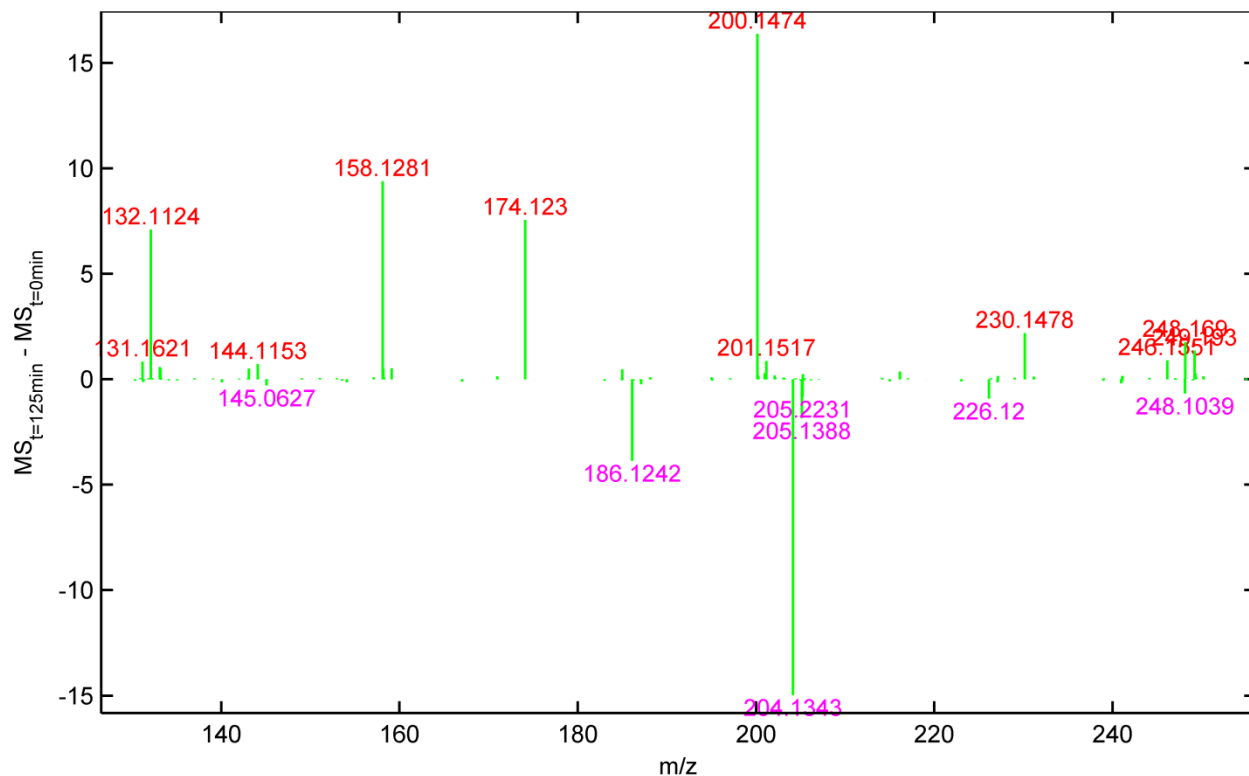


Figure S8: ESI-MS difference spectrum showing the formation of products and the disappearance of reactants from a typical glycer aldehyde photolysis experiment. The solution was photolyzed for 125 minutes.

Peak  $m/z$  was calibrated with a two point calibration using tetraethylammonium (observed at  $m/z$  130.1590 Da ) and the glycer aldehyde+GT hydrozone adduct ( $m/z$  204.1343 Da). Free GT ions appears at  $m/z$  132.1124. The product appearing at  $m/z$  158.1281 is likely the ethanal+GT hydrozone adduct while the product appearing at  $m/z$  174.123 is likely the glycolaldehyde+GT hydrozone adduct. To further confirm the presence of these products, we spiked several solutions with both ethanal and glycolaldehyde. A single hydrozone peak for each adduct was observed. Several other contaminants were consumed and products were formed. However, we were unable to unambiguously assign molecules to these species.

## 6. Reproductions of Figure 6 Under Different Atmospheric Conditions

To test how atmospheric conditions affect the identification of products that may have significant aqueous photolysis rates, four reproductions of Fig. 6 under varying atmospheric conditions are presented in Figures S9-S12. Figure S9 illustrates how solar zenith angle affects the significance of aqueous photolysis. Decreasing the solar zenith angle to its minimum value of zero degrees slightly decreases the Q value for every compound because the maximum rate of aqueous photolysis increases due to increased overlap between the actinic flux and the molar extinction coefficient. However, this decrease in SZA does not affect the conclusions of our analysis (the photolysis is slower than reactions with OH for the majority of compounds). Aqueous photolysis may be important for only two of the compounds studied in the plot: pyruvic acid and acetoacetic acid.

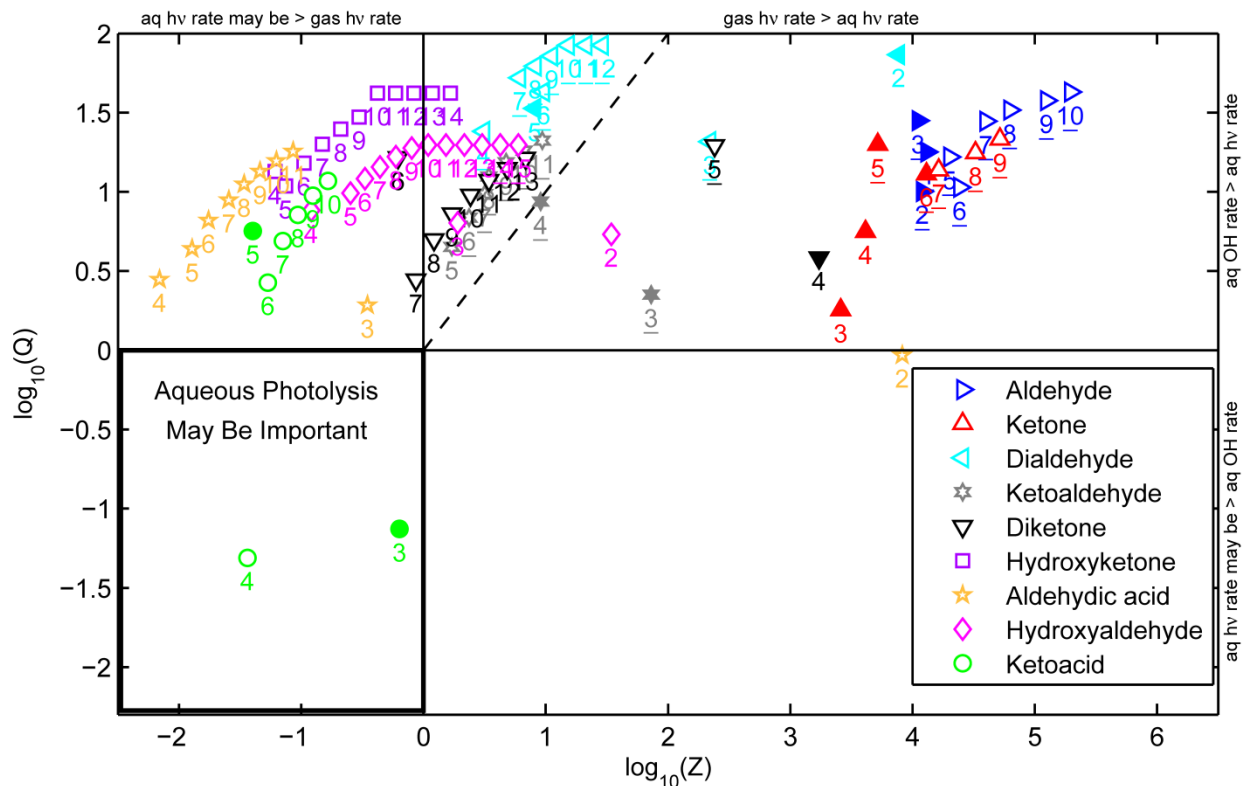


Figure S9: Reproduction of Figure 6 in the manuscript with a SZA of  $0^\circ$ . LWC =  $0.5 \text{ g m}^{-3}$ , T =  $25^\circ\text{C}$ , pH = 2, and  $C_{\text{OH}} = 10^{-13} \text{ M}$ .

The effects of decreasing the aqueous hydroxyl radical concentration to a level more commonly seen at night are illustrated in Figure S10. As in Figure S9, decreasing the aqueous OH concentration decreases the value of Q for all compounds. A few additional compounds enter the region where aqueous photolysis may be significant. However, situations where aqueous OH concentrations are  $10^{-14} \text{ M}$  with sunlight at a SZA of  $20^\circ$  are likely uncommon.

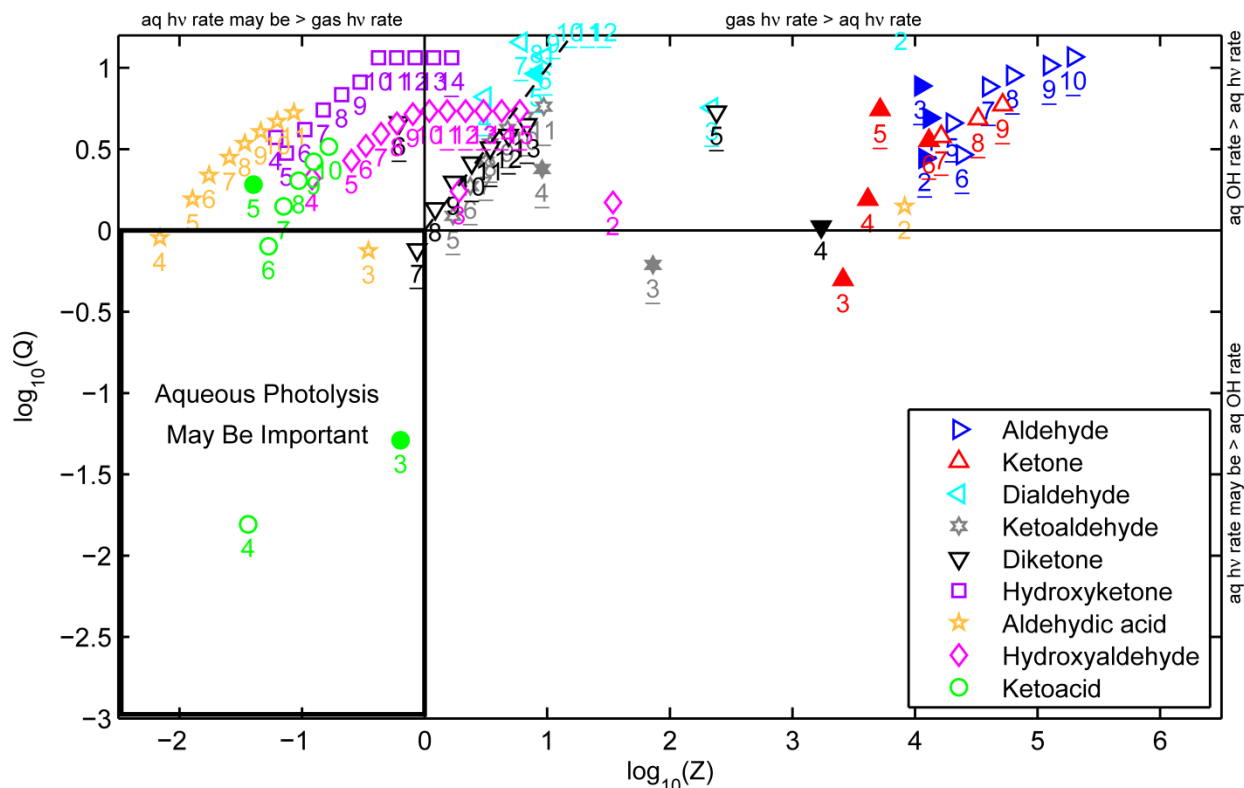


Figure S10: Reproduction of Figure 6 in the manuscript with  $C_{OH} = 2.5 \times 10^{-14}$  M. SZA is  $20^\circ$ ,  $LWC = 0.5 \text{ g m}^{-3}$ ,  $T = 25^\circ\text{C}$ , and  $\text{pH} = 2$ .

Figure S11 details the effects of changing the LWC to  $0.05 \text{ g m}^{-3}$ . The lower LWC value increases the significance of the gas-phase processes. Pyruvic acid moves into the region where gaseous photolysis is the most significant sink.

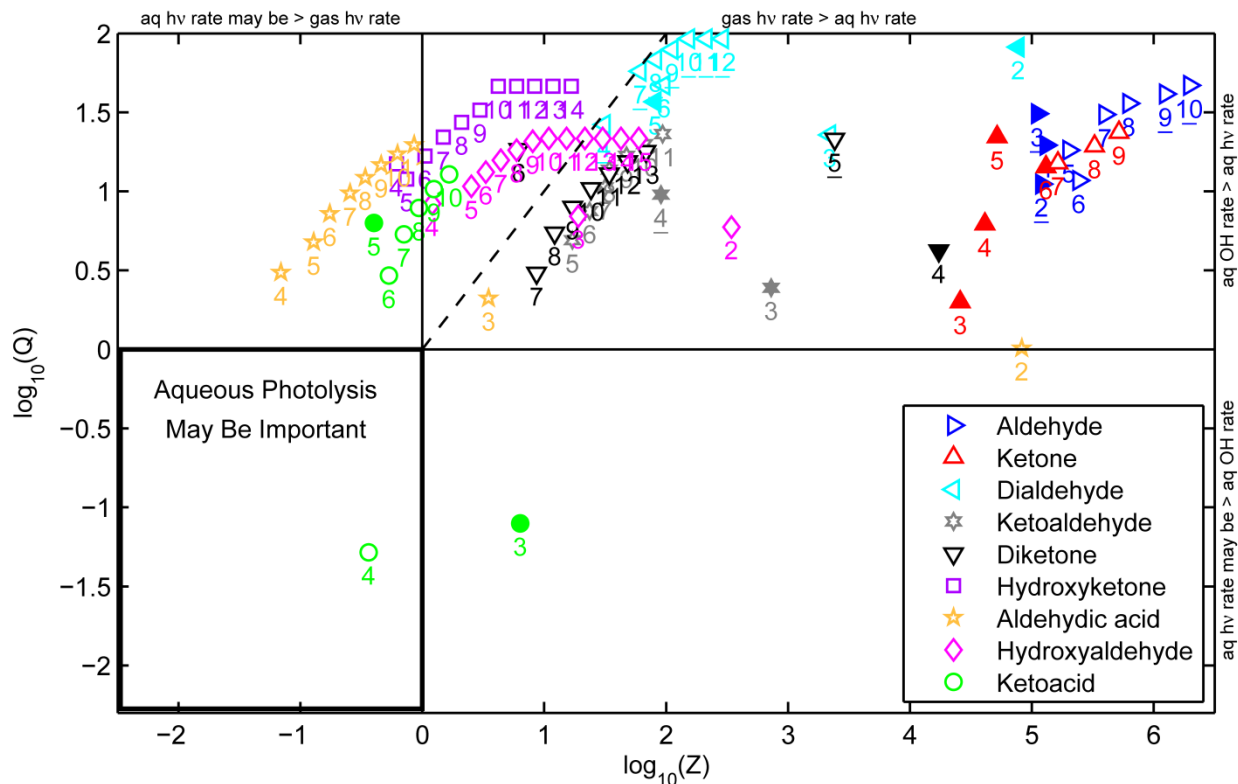


Figure S11: Reproduction of Figure 6 in the manuscript with  $LWC = 0.05 \text{ g m}^{-3}$ ,  $SZA$  is  $20^\circ$ ,  $T = 25^\circ\text{C}$ ,  $\text{pH} = 2$ , and  $C_{\text{OH}} = 10^{-13} \text{ M}$ .

Figure S12 shows how cloud-water acidity affects the fate of aldehydic acids and ketoacids. Changing the cloud-water acidity from a pH of 2 to a pH of 6 does not significantly change the chemical behavior of the acids investigated.

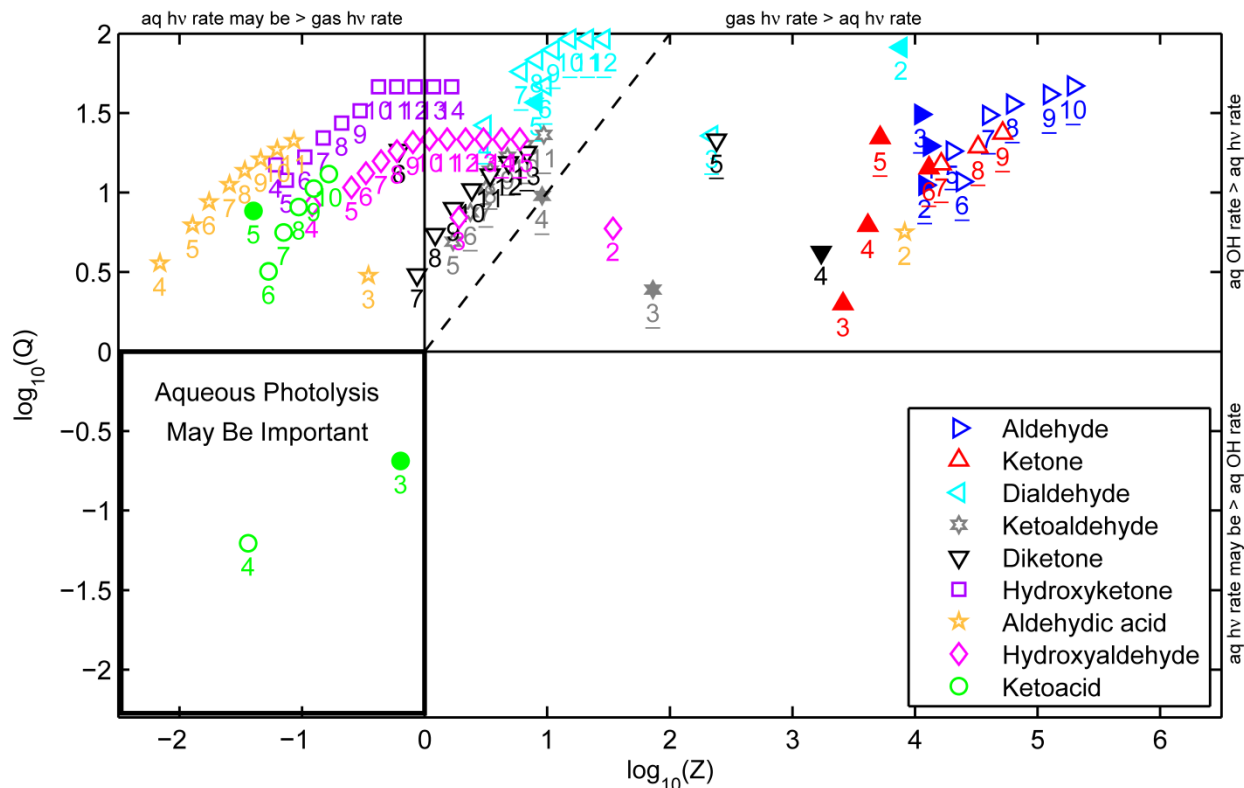


Figure S12: Reproduction of Figure 6 in the manuscript with pH = 6. SZA is  $20^\circ$ , LWC =  $0.5 \text{ g m}^{-3}$ ,  $T = 25^\circ\text{C}$ , and  $C_{\text{OH}} = 10^{-13} \text{ M}$ .

We also investigated the uncertainties in  $Q$  and  $Z$  that arise from using estimates of  $K_{\text{H}}$ ,  $K_{\text{hyd}}$ ,  $k_{\text{OH}}$ , and  $\text{p}K_{\text{A}}$  in the absence of experimental data. Uncertainties in  $Z$  are a function of root-mean-square deviations between predicted and experimental  $K_{\text{hyd}}$  values from (Hilal et al., 2005) and standard deviations from bond and group method  $K_{\text{H}}$  predictions (EPA, 2011). Uncertainties in  $Q$  are a function of the uncertainties in predicting  $k_{\text{OH}}$  values from the (Doussin and Monod, 2013) SAR and the prediction uncertainty between photolysis rates calculated with the entire UV-extinction coefficients and photolysis rates calculated with  $\lambda_{\text{max}}$  and  $\epsilon_{\text{max}}$ . Photolysis rate prediction uncertainties were obtained from a comparison of rates calculated for eight carbonyl compounds with experimentally determined extinction coefficients from (Xu et al., 1993) and this work: ethanal, propanal, butanal, acetone, butanone, 2-pentanone, dihydroxyacetone, and glyceraldehyde (see Figure S14). For purposes of this analysis, compounds with experimental parameters were assigned an uncertainty of zero. Figure S13 displays uncertainties in  $Q$  and  $Z$  parameters.

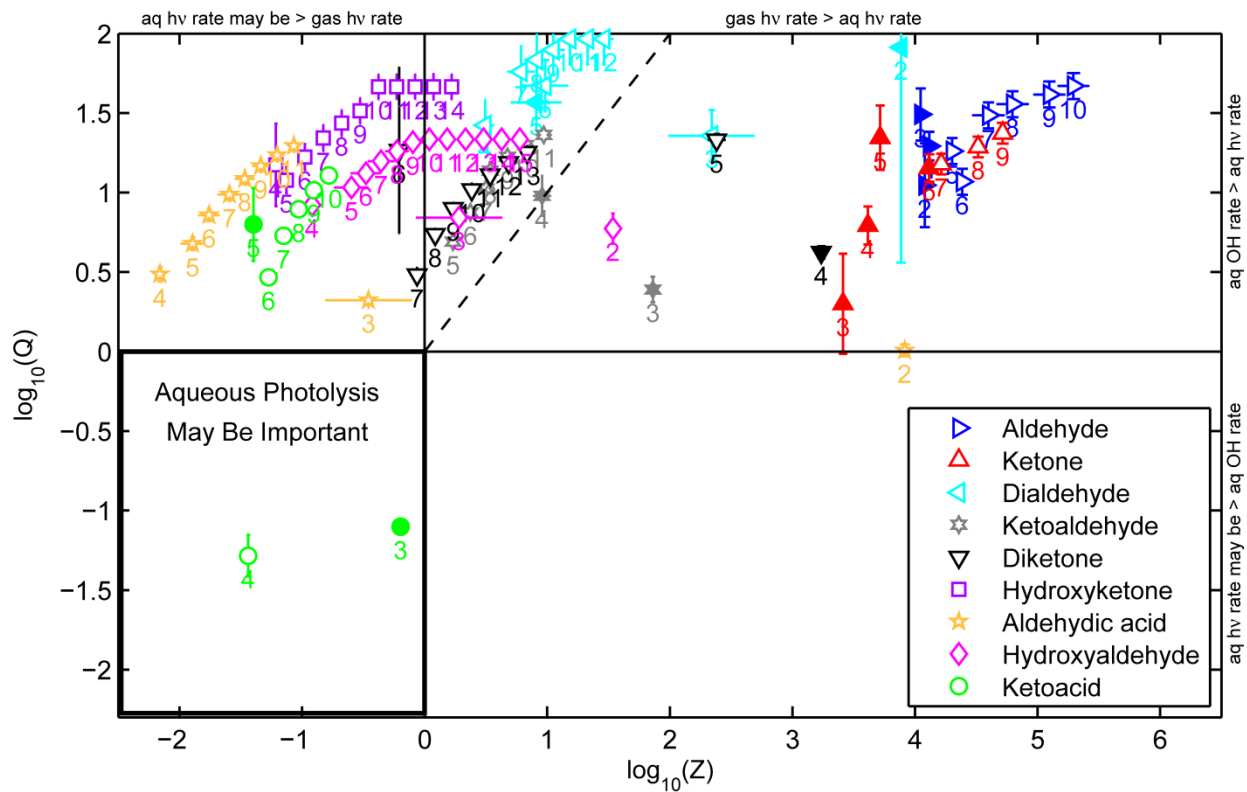


Figure S13: Uncertainty estimates in the parameters Q and Z arising from calculations of model parameters



## 7. Literature Values for $\epsilon_{\max}$ and $\lambda_{\max}$

The literature values used to generate Figure 6 and Figures S9-S12 are presented in Table S1 below. Structures for the first three molecules in each series are presented in Table S2.

Table S1:  $\epsilon_{\max}$  and  $\lambda_{\max}$  values used to determine aqueous photolysis rates for Figures 6, and S9-S12. The upper row indicates the total number of carbon atoms in a molecule with a functionality specified by the first column. Bold values were obtained from the literature with subscripted reference numbers: Ref 1 (Mackinney and Temmer, 1948); Ref 2 (Xu et al., 1993); Ref 3 (Rice, 1920); Ref 4 (Malik and Joens, 2000); Ref 5 (Schutze and Herrmann, 2004); Ref 6 (Martinez et al., 1975); Ref 7(Gubina et al., 2004); Ref 8 (Steenken et al., 1975); Ref 9 (Maroni, 1957); Ref 10 (Beeby et al., 1987). For compounds without published data, an upper estimate was used based on the properties of molecules with similar functionalities.

# C atoms	$\Rightarrow$	2	3	4	5	6	7	8	9	10	11	12	13	14	15
Aldehyde	$\epsilon_{\max}$	<b>8.1<sub>1</sub></b>	<b>13.1<sub>1</sub></b>	<b>13.5<sub>1</sub></b>	15	15	15	15	15	15	15	15	15	15	15
	$\lambda_{\max}$	<b>277.5<sub>1</sub></b>	<b>277.5<sub>1</sub></b>	<b>282.5<sub>1</sub></b>	282.5	282.5	282.5	282.5	282.5	282.5	282.5	282.5	282.5	282.5	282.5
Ketone	$\epsilon_{\max}$		<b>17.6<sub>2</sub></b>	<b>17.9<sub>2</sub></b>	<b>24<sub>2</sub></b>	<b>21.2<sub>3</sub></b>	25	25	25	25	25	25	25	25	25
	$\lambda_{\max}$		<b>264<sub>2</sub></b>	<b>277.5<sub>2</sub></b>	<b>271<sub>2</sub></b>	<b>279<sub>3</sub></b>	280	280	280	280	280	280	280	280	280
Dialdehyde	$\epsilon_{\max}$	<b>5.8<sub>1</sub></b>	8	8	<b>7.9<sub>4</sub></b>	8	8	8	8	8	8	8	8	8	8
	$\lambda_{\max}$	<b>267.5<sub>1</sub></b>	282	282	<b>282<sub>4</sub></b>	282	282	282	282	282	282	282	282	282	282
Keto-aldehyde	$\epsilon_{\max}$		<b>16<sub>5</sub></b>	<b>13<sub>6</sub></b>	20	20	20	20	20	20	20	20	20	20	20
	$\lambda_{\max}$		<b>284<sub>5</sub></b>	<b>280<sub>6</sub></b>	285	285	285	285	285	285	285	285	285	285	285
Diketone	$\epsilon_{\max}$			<b>26.5<sub>5</sub></b>	25	25	25	25	25	25	25	25	25	25	25
	$\lambda_{\max}$			<b>284<sub>5</sub></b>	285	<b>264<sub>7</sub></b>	285	285	285	285	285	285	285	285	285
Hydroxy-ketone	$\epsilon_{\max}$		<b>20<sub>8</sub></b>	20	20	20	20	20	20	20	20	20	20	20	20
	$\lambda_{\max}$		<b>267<sub>8</sub></b>	<b>270.5<sub>9</sub></b>	280	280	280	280	280	280	280	280	280	280	280
Acid-aldehyde	$\epsilon_{\max}$	25	25	25	25	25	25	25	25	25	25	25	25	25	25
	$\lambda_{\max}$	285	285	285	285	285	285	285	285	285	285	285	285	285	285
Hydroxy-aldehyde	$\epsilon_{\max}$	25	25	25	25	25	25	25	25	25	25	25	25	25	25
	$\lambda_{\max}$	<b>277<sub>10</sub></b>	285	285	285	285	285	285	285	285	285	285	285	285	285
Ketoacid	$\epsilon_{\max}$		<b>19.5<sub>1</sub></b>	25	<b>25.1<sub>1</sub></b>	25	25	25	25	25	25	25	25	25	25
	$\lambda_{\max}$		<b>317.5<sub>1</sub></b>	317.5	<b>270<sub>1</sub></b>	285	285	285	285	285	285	285	285	285	285

Table S2: Structures corresponding to the molecules listed in Table S1. As described in the text, functional groups occupy the terminal positions in the chain.

	C# = 1	C# = 2	C# = 3	C# = 4	C# = 5	C# = 6
Aldehyde						
Ketone	N/A	N/A				
Dialdehyde	N/A					
Ketoaldehyde	N/A	N/A				
Diketone	N/A	N/A	N/A			
Hydroxyketone	N/A	N/A				
Aldehydic Acid	N/A					
Hydroxyaldehyde	N/A					
Keto Acid	N/A	N/A				

## 8. Evaluation of the Aqueous Photolysis Rate Constant Parameterization

Figure S14 compares Q-values calculated with published extinction coefficients and Q-values calculated with our  $\lambda_{\max}$  and  $\epsilon_{\max}$  parameterization. The parameterization performs reasonably well for simple carbonyls. Parameterized Q-values have acceptable uncertainties for our order-of-magnitude analysis.

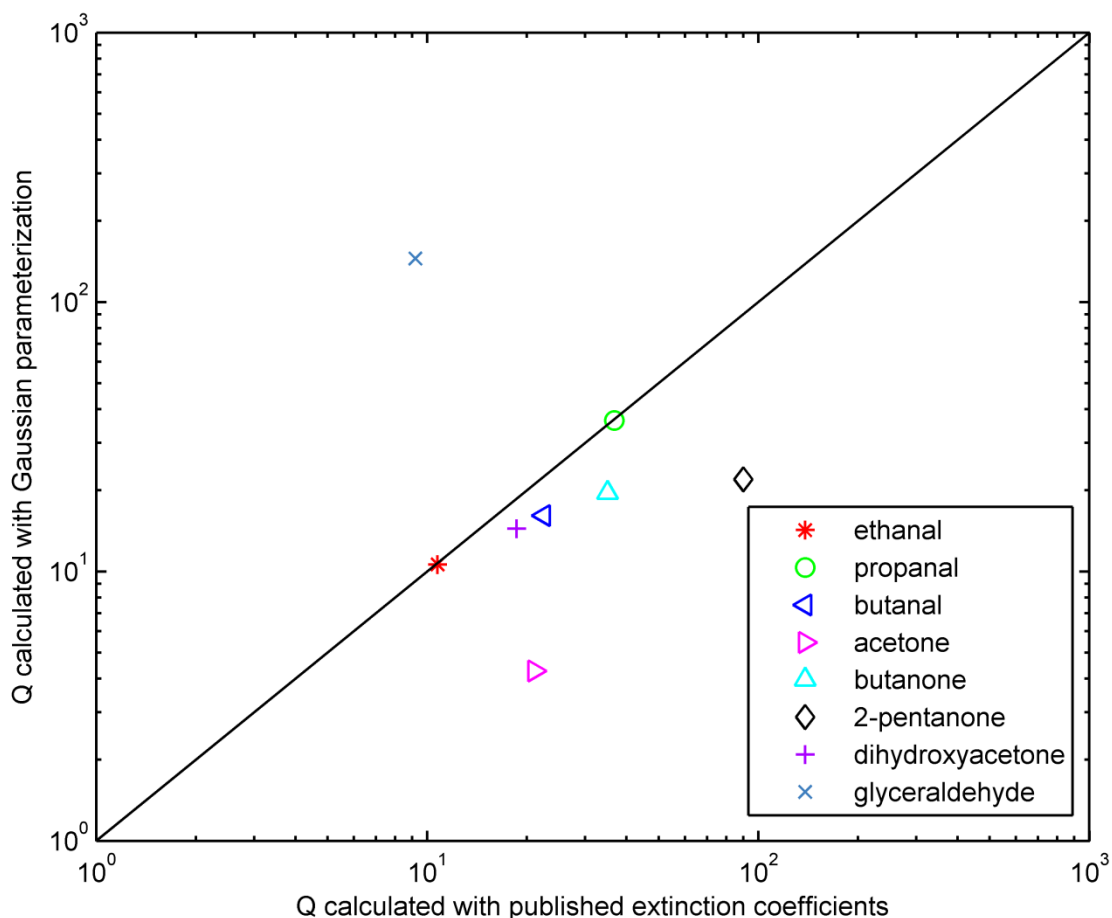


Figure S14: Comparison of Q-values calculated with published extinction coefficients as a function of wavelength and Q-values calculated with our  $\lambda_{\max}$  and  $\epsilon_{\max}$  parameterization

### 9. Comparing Aqueous Photolysis with Aqueous Oxidation by OH at a pH of 6

Figure 5 in the manuscript was reproduced with a pH of 6. Since we do not account for the effects of pH on hydration, only the acids (levulinic acid and pyruvic acid) were affected. A higher pH increased the fraction of anion in solution leading to increased rates of oxidation by OH. However, the increase in the rate of pyruvic acid oxidation is not large enough to exceed the maximum rate of aqueous photolysis.

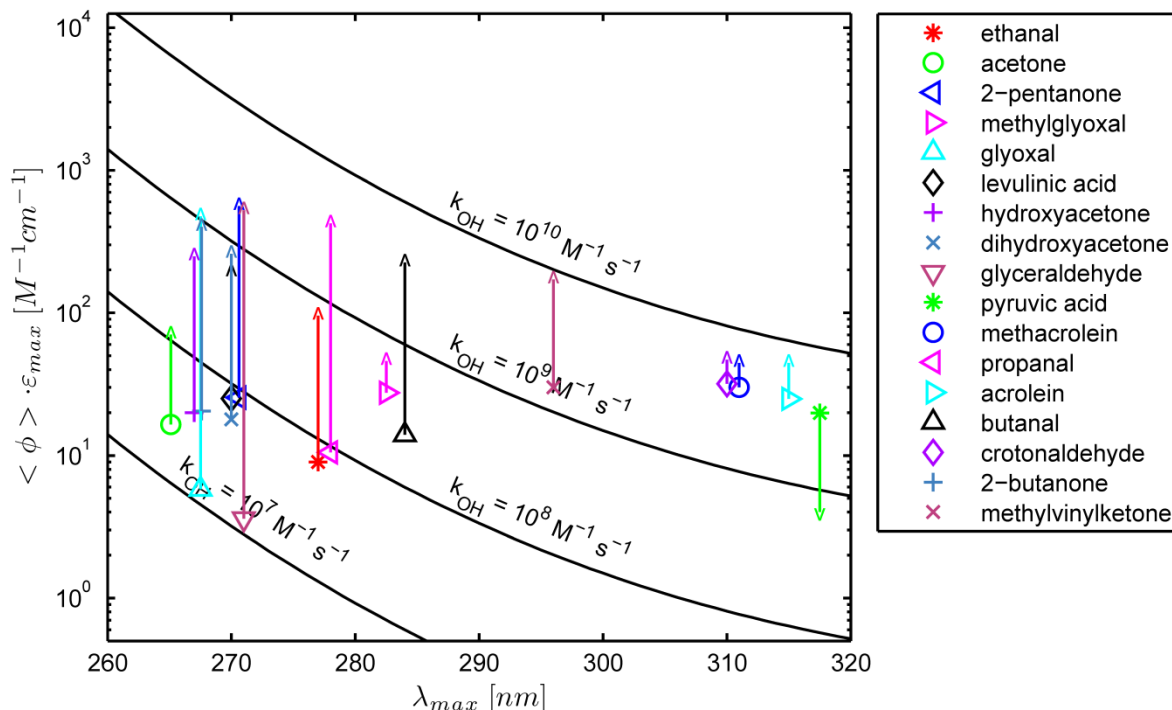


Figure S15: Comparison of aqueous photolysis at a solar zenith angle of  $20^\circ$  and aqueous oxidation by OH at a typical daytime concentration of  $10^{-13}$  M and a pH of 6. Molecules, denoted by the markers in the key, have arrows that point to their corresponding  $k_{OH}$ .  $k_{OH}$  isopleths correspond to  $\lambda_{max}$  and  $\epsilon_{max} \cdot \langle \Phi \rangle$  values where  $Q = 1$ . Molecules with values of  $\lambda_{max}$  and  $\epsilon_{max} \cdot \langle \Phi \rangle$  that are below their corresponding  $k_{OH}$  value will be preferentially removed with oxidation by OH. Conversely, molecules with values of  $\lambda_{max}$  and  $\epsilon_{max} \cdot \langle \Phi \rangle$  that are above their corresponding  $k_{OH}$  value will be preferentially removed by aqueous photolysis.

## 10. Predicted $k_{OH}$ as a Function of Molecular Structure

Figure S16 shows how SAR-predicted  $k_{OH}$  values vary with carbon number for the carbonyls investigated. For purposes of this illustration, all points were calculated with SAR.  $k_{OH}$  values increase as carbons with additional abstractable protons are added. Diketones have the lowest rate constants for their corresponding carbon number. This is due to the deactivating ketone functionality. Hydroxyaldehydes have the largest rate constants for their corresponding carbon number due to the activating effects of an alcohol group on adjacent hydrogen atoms and the relative ease of abstracting an aldehydic hydrogen. Rate constants are capped at their diffusion limited value taken as  $10^{10}$  L mol $^{-1}$  s $^{-1}$ .

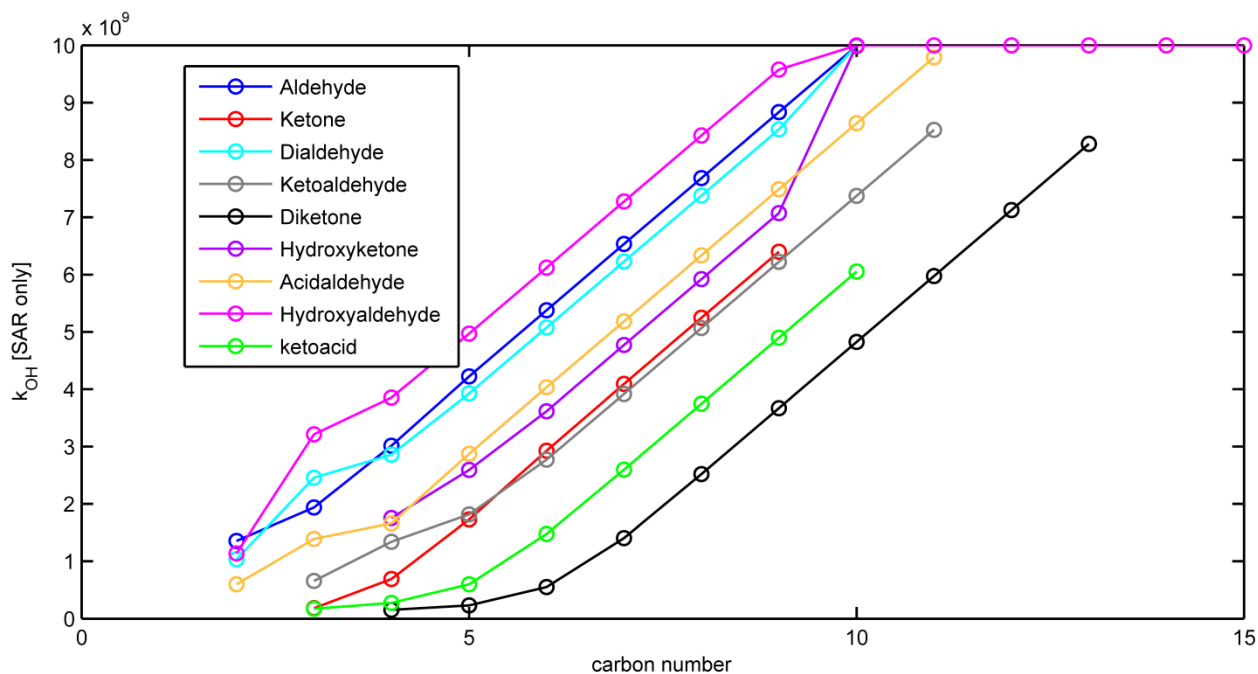


Figure S16: Aqueous rate constants for oxidation by OH as a function of carbon number (in the units of  $\text{L mol}^{-1} \text{s}^{-1}$ ). All rate constants were predicted with SAR developed by (Doussin and Monod, 2013) and (Monod and Doussin, 2008).

Figure S17 illustrates how the number of hydrogens affects  $k_{\text{OH}}$  values. As expected,  $k_{\text{OH}}$  values increase with increasing hydrogen number. The number of hydrogen atoms is a slightly better indicator of the value of  $k_{\text{OH}}$  as the hydrogen number vs.  $k_{\text{OH}}$  curves are closer together than the carbon number vs.  $k_{\text{OH}}$  curves in Figure S16.

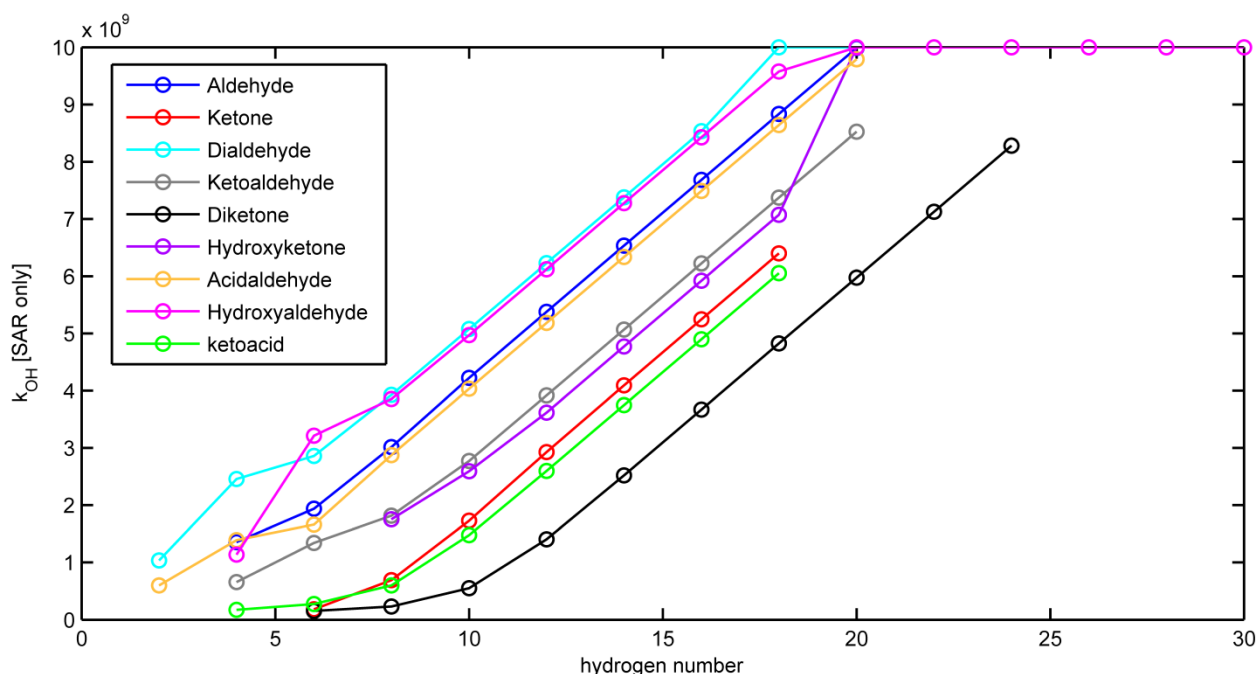


Figure S17: Aqueous rate constants for oxidation by OH as a function of hydrogen number. All rate constants were predicted with SAR developed by (Doussin and Monod, 2013) and (Monod and Doussin, 2008).

## 11. Computational Analysis of Additional Atmospherically Relevant Compounds

We chose four additional compounds to study that were identified in d-limonene (Fang et al., 2012) and isoprene (Jaoui et al., 2006) SOA. The computational methods and results are detailed in the text. Table S3 contains the calculated  $\epsilon_{\max}$  and  $\lambda_{\max}$  values.

Table S3: Calculated  $\epsilon_{\max}$  and  $\lambda_{\max}$  values for compounds found in d-limonene and isoprene SOA. Both 3,6-oxoheptanoic acid and ketolimonanaldehyde have two peaks on their calculated spectra.

Structure	Name	Reference	$\lambda_{\max}$ [nm]	$\epsilon_{\max}$ [ $M^{-1} cm^{-1}$ ]
	4-hydroxy-3-methyl-but-2-enal	(Fang et al., 2012)	276	493.4
	3,6-oxoheptanoic acid	(Jaoui et al., 2006)	286/304	162.3/5.7
	ketolimononaldehyde	(Jaoui et al., 2006)	296/299	179.7/192.5
	ketonorlimonic acid	(Jaoui et al., 2006)	275	88.5

## 12. Molecular Dynamics Simulation of Molar Extinction Plots

TDDFT predictions of molar extinction as a function of wavelength for all compounds investigated with computational methods are presented in Figures S18-S27. Lower energy peaks in the visible region are predicted for dicarbonyls with adjacent carbonyl groups (biacetyl and methyl glyoxal). Strong exciton splitting of  $\pi^* \leftarrow n$  excitations result in an additional absorption band. This secondary  $\pi^* \leftarrow n$  band is present in experimental spectra of biacetyl (Cohen et al., 1948) and methyl glyoxal (Staffelbach et al., 1995). Quantum yields are typically significantly lower in the visible range than in the UV, but the enhanced actinic flux may make photolysis in the visible important.

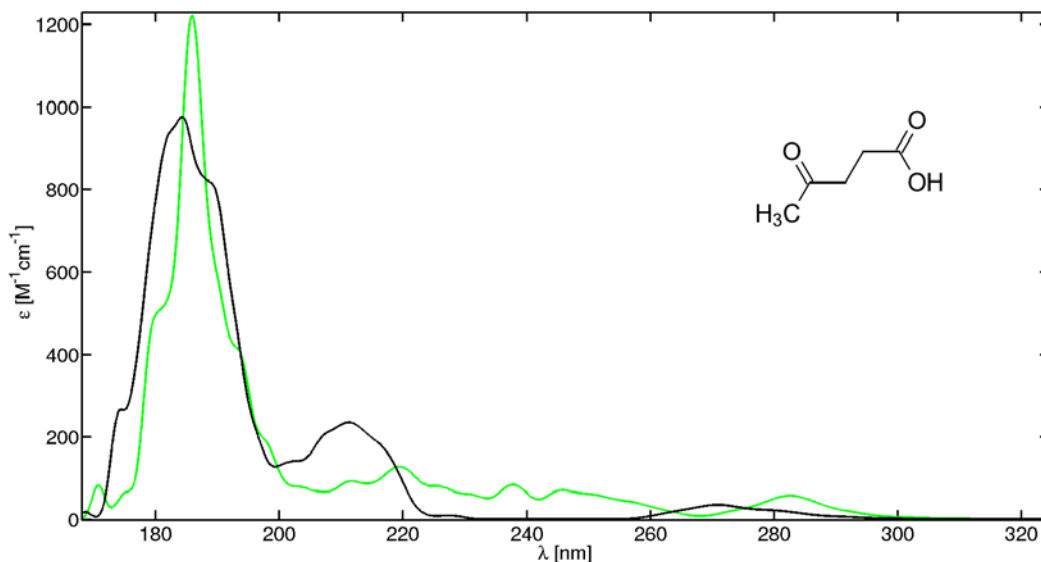


Figure S18: Calculated MD extinction coefficients for gaseous (green) and aqueous (black) levulinic acid [4-oxopentanoic acid].

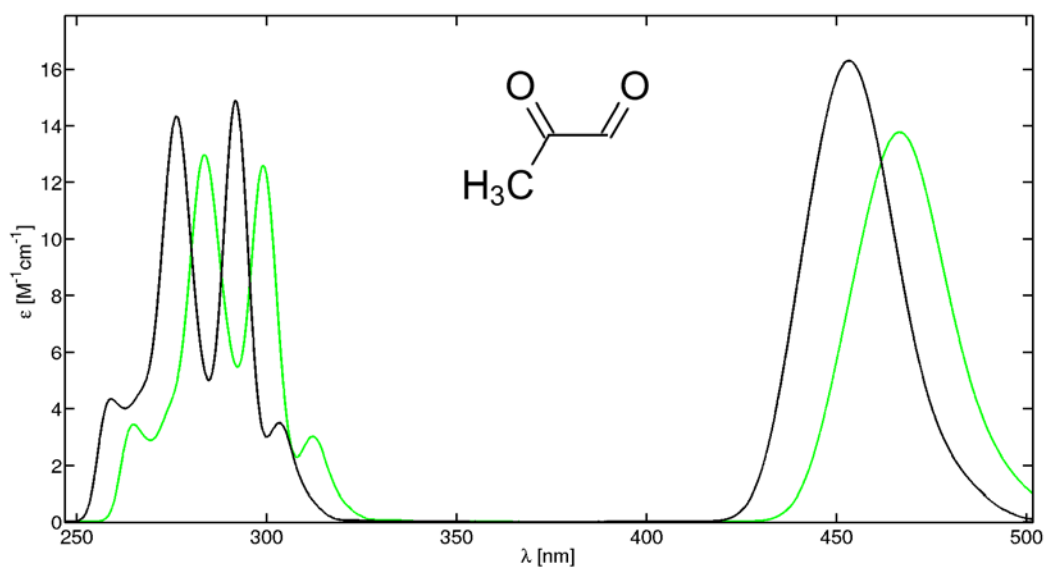


Figure S19: Calculated MD extinction coefficients for gaseous (green) and aqueous (black) methyl glyoxal [2-oxopropanal].

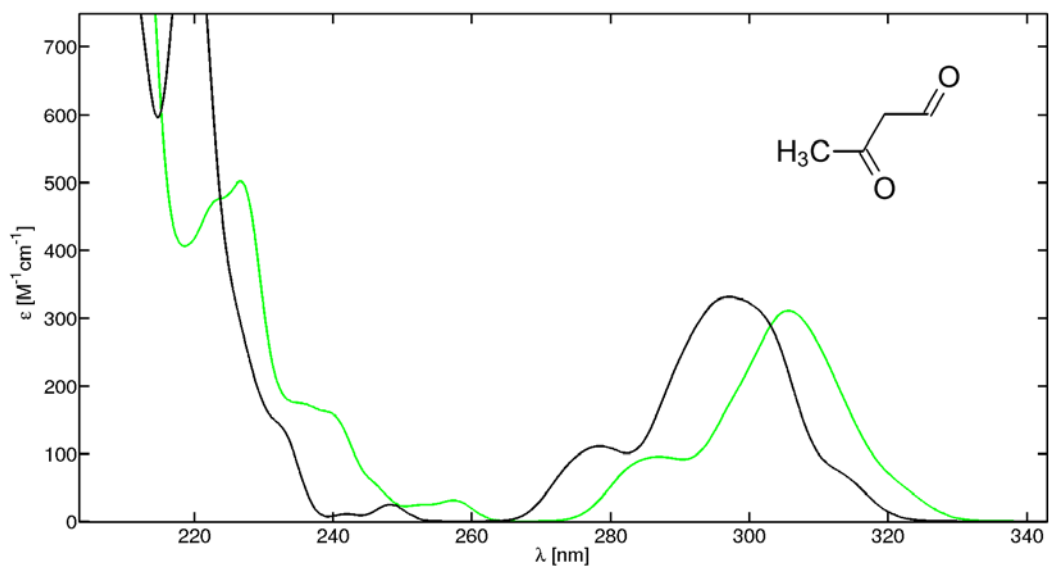


Figure S20: Calculated MD extinction coefficients for gaseous (green) and aqueous (black) 3-oxobutanal.



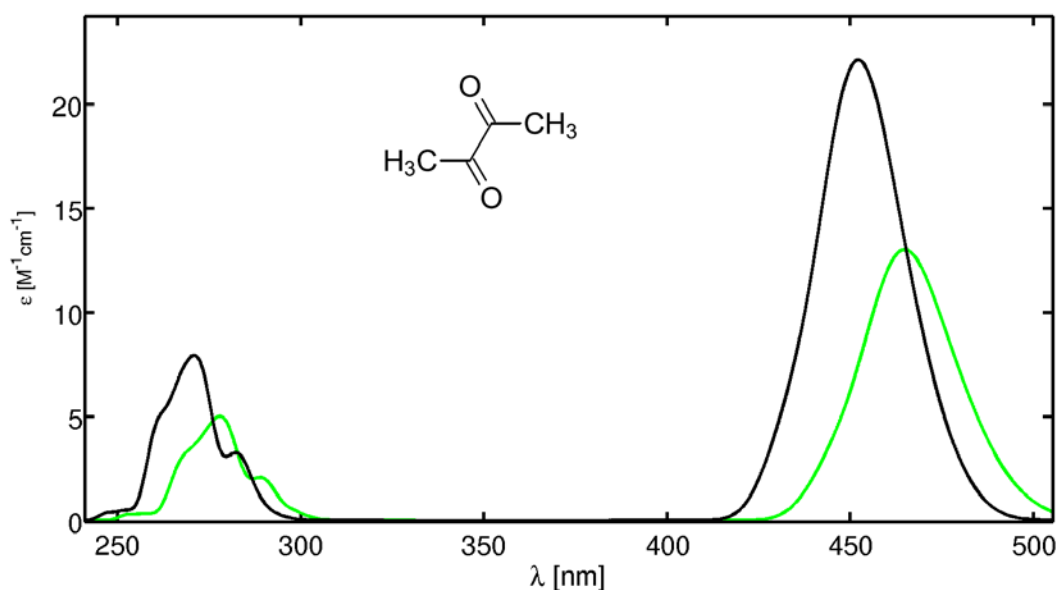


Figure S21: Calculated MD extinction coefficients for gaseous (green) and aqueous (black) biacetyl [2,3-butanedione].

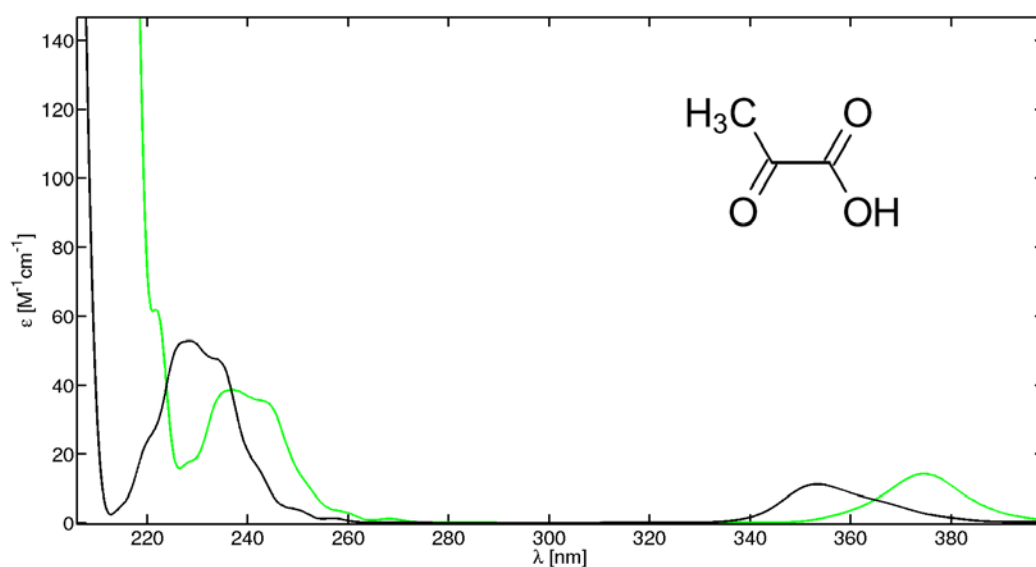


Figure S22: Calculated MD extinction coefficients for gaseous (green) and aqueous (black) pyruvic acid [2-oxopropanoic acid].

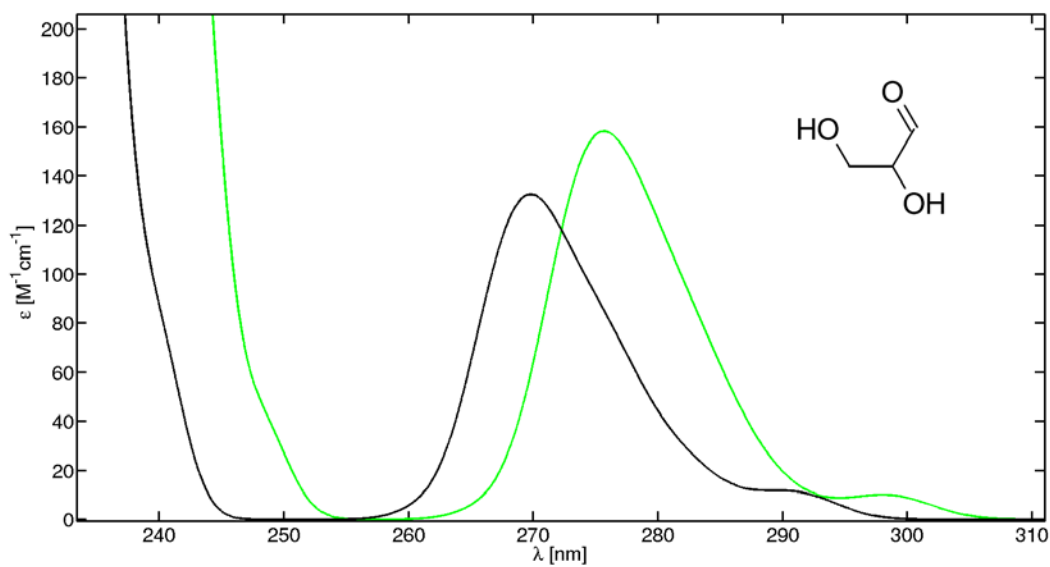


Figure S23: Calculated MD extinction coefficients for gaseous (green) and aqueous (black) glyceraldehyde [2,3-dihydroxypropanal].

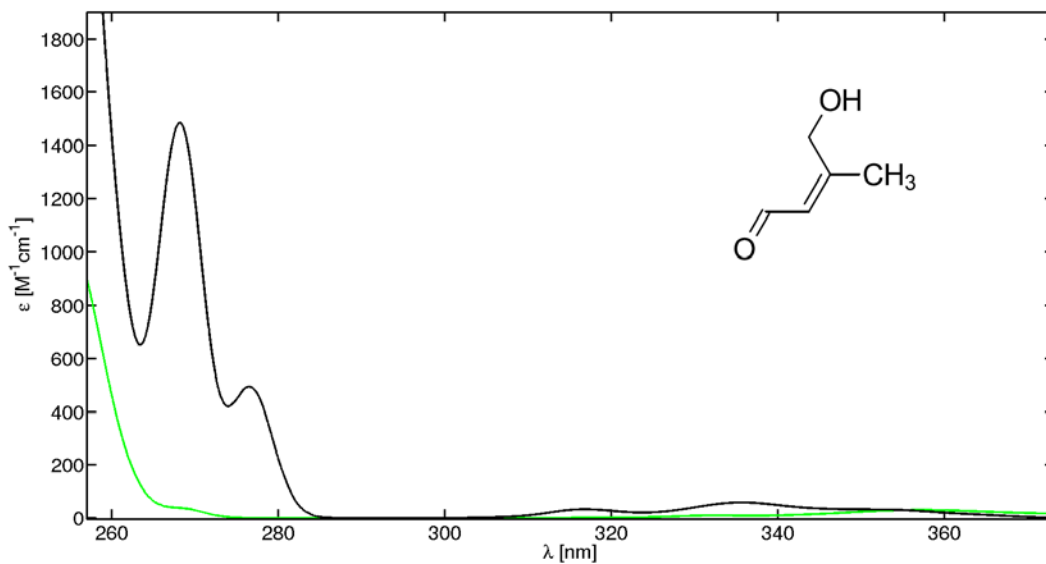


Figure S24: Calculated MD extinction coefficients for gaseous (green) and aqueous (black) 4-hydroxy-3-methyl-but-2-enal.

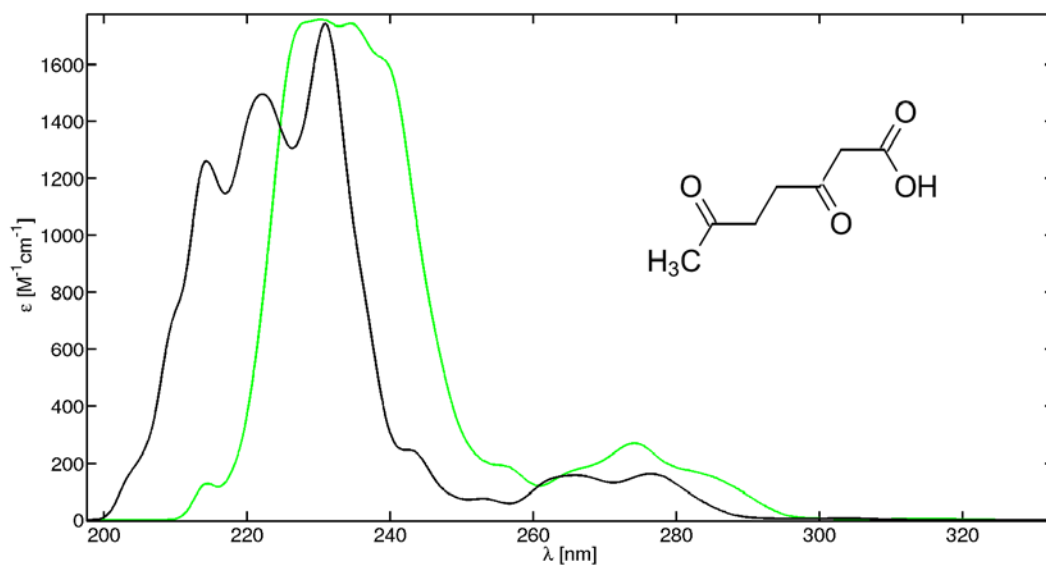


Figure S25: Calculated MD extinction coefficients for gaseous (green) and aqueous (black) 3,6-dioxoheptanoic acid.

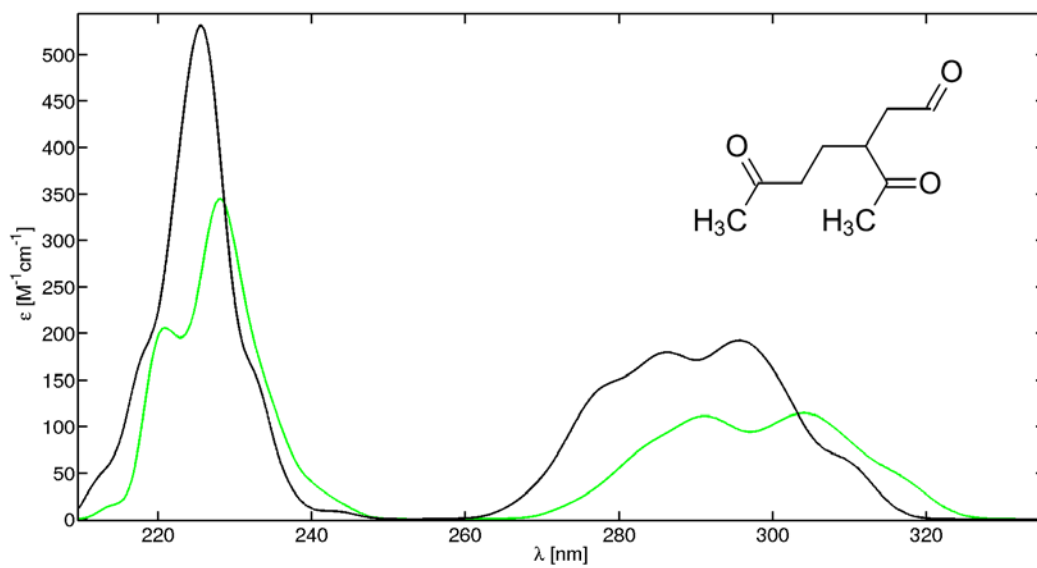


Figure S26: Calculated MD extinction coefficients for gaseous (green) and aqueous (black) ketolimonaldehyde.

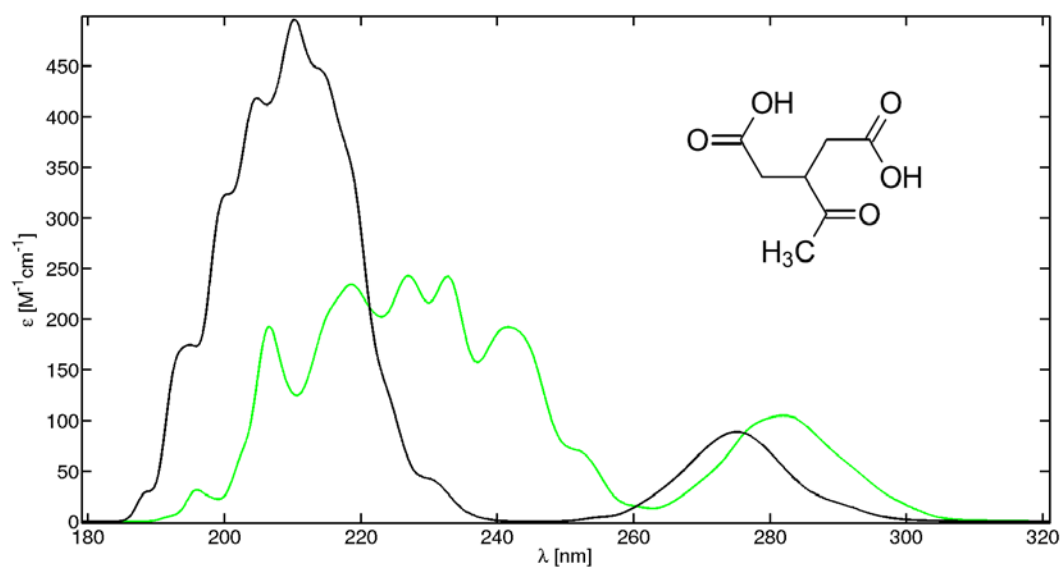


Figure S27: Calculated MD extinction coefficients for gaseous (green) and aqueous (black) ketonorlimonic acid.

### 13. Tabular Extinction Coefficients of Glyceraldehyde and Dihydroxyacetone

Table S4: Measured extinction coefficients of glyceraldehyde in terms of total (free + hydrated) concentration (i.e., decadal absorbance = total concentration  $\times$  pathlength  $\times$  extinction coefficient listed in the table). The uncertainties arise from the linear least-squares regression of concentration vs. absorbance when determining the extinction coefficient.

wavelength (nm)	Extinction (1/M/cm)	uncertainty in Extinction (1/M/cm)	wavelength (nm)	Extinction (1/M/cm)	uncertainty in Extinction (1/M/cm)
200	20.53	0.34	241	3.08	0.02
201	18.95	0.31	242	3.08	0.02
202	17.51	0.28	243	3.08	0.02
203	16.18	0.25	244	3.08	0.02
204	14.95	0.23	245	3.08	0.02
205	13.86	0.22	246	3.08	0.02
206	12.82	0.21	247	3.09	0.02
207	11.92	0.20	248	3.10	0.02
208	11.10	0.19	249	3.10	0.02
209	10.40	0.19	250	3.10	0.02
210	9.69	0.18	251	3.11	0.02
211	9.07	0.17	252	3.12	0.02
212	8.54	0.16	253	3.14	0.01
213	8.04	0.15	254	3.16	0.02
214	7.57	0.14	255	3.18	0.02
215	7.14	0.13	256	3.20	0.02
216	6.71	0.12	257	3.23	0.02
217	6.34	0.11	258	3.27	0.02
218	5.98	0.10	259	3.30	0.02
219	5.67	0.09	260	3.34	0.02
220	5.36	0.08	261	3.38	0.02
221	5.09	0.07	262	3.42	0.02
222	4.84	0.06	263	3.46	0.02
223	4.59	0.06	264	3.50	0.03
224	4.36	0.06	265	3.54	0.02
225	4.12	0.05	266	3.58	0.02
226	3.91	0.04	267	3.61	0.02
227	3.72	0.04	268	3.64	0.02
228	3.56	0.04	269	3.65	0.02
229	3.44	0.04	270	3.67	0.02
230	3.33	0.03	271	3.68	0.02
231	3.27	0.03	272	3.67	0.03
232	3.21	0.03	273	3.66	0.03
233	3.17	0.03	274	3.65	0.03
234	3.15	0.03	275	3.62	0.02
235	3.13	0.02	276	3.59	0.02
236	3.11	0.02	277	3.55	0.02
237	3.10	0.02	278	3.50	0.03
238	3.09	0.02	279	3.46	0.02
239	3.09	0.02	280	3.40	0.02
240	3.08	0.02	281	3.33	0.02

Table S4: Measured extinction coefficients of glyceraldehyde (continued).

wavelength (nm)	Extinction (1/M/cm)	uncertainty in Extinction (1/M/cm)	wavelength (nm)	Extinction (1/M/cm)	uncertainty in Extinction (1/M/cm)
282	3.26	0.02	324	0.63	0.00
283	3.19	0.02	325	0.60	0.00
284	3.12	0.02	326	0.57	0.00
285	3.04	0.02	327	0.55	0.00
286	2.96	0.02	328	0.52	0.00
287	2.88	0.02	329	0.50	0.00
288	2.79	0.02	330	0.48	0.00
289	2.70	0.02	331	0.46	0.00
290	2.61	0.02	332	0.44	0.00
291	2.52	0.01	333	0.42	0.00
292	2.43	0.01	334	0.41	0.00
293	2.33	0.01	335	0.40	0.00
294	2.24	0.01	336	0.38	0.00
295	2.16	0.01	337	0.36	0.00
296	2.07	0.01	338	0.35	0.00
297	1.99	0.01	339	0.34	0.01
298	1.90	0.01	340	0.33	0.00
299	1.82	0.01	341	0.32	0.00
300	1.74	0.01	342	0.31	0.00
301	1.67	0.01	343	0.30	0.00
302	1.60	0.01	344	0.29	0.00
303	1.53	0.01	345	0.28	0.00
304	1.46	0.01	346	0.27	0.00
305	1.40	0.00	347	0.27	0.00
306	1.33	0.01	348	0.26	0.00
307	1.27	0.00	349	0.26	0.00
308	1.22	0.00	350	0.25	0.00
309	1.17	0.00	351	0.24	0.00
310	1.12	0.00	352	0.24	0.00
311	1.07	0.00	353	0.24	0.01
312	1.03	0.00	354	0.23	0.00
313	0.99	0.01	355	0.22	0.00
314	0.95	0.00	356	0.22	0.00
315	0.91	0.00	357	0.22	0.01
316	0.87	0.00	358	0.21	0.00
317	0.84	0.00	359	0.21	0.00
318	0.80	0.00	360	0.20	0.00
319	0.77	0.00	361	0.20	0.00
320	0.74	0.00	362	0.20	0.00
321	0.71	0.00	363	0.19	0.01
322	0.68	0.00	364	0.19	0.01
323	0.65	0.00	365	0.19	0.00

Table S4: Measured extinction coefficients of glyceraldehyde (continued).

wavelength (nm)	Extinction (1/M/cm)	uncertainty in Extinction (1/M/cm)
366	0.18	0.00
367	0.18	0.00
368	0.17	0.00
369	0.17	0.01
370	0.17	0.01
371	0.16	0.00
372	0.16	0.00
373	0.16	0.00
374	0.16	0.00
375	0.15	0.00
376	0.15	0.00
377	0.15	0.00
378	0.14	0.01
379	0.14	0.00
380	0.14	0.00
381	0.14	0.00
382	0.13	0.00
383	0.13	0.00
384	0.12	0.00
385	0.12	0.00
386	0.12	0.00
387	0.12	0.00
388	0.12	0.00
389	0.12	0.00
390	0.11	0.00
391	0.11	0.00
392	0.11	0.00
393	0.11	0.00
394	0.11	0.00
395	0.10	0.00
396	0.10	0.00
397	0.10	0.00
398	0.10	0.00
399	0.09	0.00
400	0.09	0.00

Table S5: Measured extinction coefficients of dihydroxyacetone in terms of total (free + hydrated) concentration. The uncertainties arise from the linear least-squares regression of concentration vs. absorbance when determining the extinction coefficient.

wavelength (nm)	Extinction (1/M/cm)	uncertainty in Extinction (1/M/cm)	wavelength (nm)	Extinction (1/M/cm)	uncertainty in Extinction (1/M/cm)
200	6.32	0.20	284	13.53	0.03
202	8.04	1.12	286	12.31	0.03
204	13.45	4.17	288	11.11	0.04
206	21.12	6.43	290	9.81	0.04
208	27.16	4.04	292	8.53	0.06
210	25.43	0.74	294	7.27	0.02
212	18.37	0.14	296	6.10	0.04
214	12.37	0.07	298	5.06	0.04
216	8.06	0.09	300	4.10	0.03
218	5.24	0.06	302	3.28	0.01
220	3.50	0.04	304	2.61	0.02
222	2.50	0.03	306	1.94	0.01
224	1.98	0.03	308	1.47	0.01
226	1.81	0.01	310	1.07	0.01
228	1.88	0.02	312	0.81	0.01
230	2.14	0.01	314	0.58	0.01
232	2.52	0.00	316	0.42	0.01
234	2.98	0.01	318	0.30	0.02
236	3.55	0.01	320	0.22	0.01
238	4.26	0.02	322	0.17	0.01
240	5.08	0.01	324	0.12	0.00
242	6.00	0.03	326	0.09	0.01
244	6.95	0.04	328	0.07	0.02
246	8.00	0.01	330	0.06	0.01
248	9.07	0.02	332	0.03	0.01
250	10.19	0.02	334	0.04	0.01
252	11.34	0.02	336	0.02	0.01
254	12.45	0.03	338	0.03	0.01
256	13.58	0.01	340	0.00	0.00
258	14.59	0.03	342	0.02	0.01
260	15.51	0.04	344	0.00	0.01
262	16.32	0.04	346	0.03	0.01
264	17.00	0.03	348	0.01	0.01
266	17.54	0.01	350	0.01	0.01
268	17.81	0.02	352	0.02	0.01
270	17.95	0.02	354	0.02	0.01
272	17.83	0.02	356	0.01	0.01
274	17.56	0.03	358	0.02	0.01
276	17.12	0.05	360	0.02	0.02
278	16.43	0.04	362	0.00	0.00
280	15.58	0.04	364	0.02	0.01
282	14.63	0.04	366	0.00	0.01



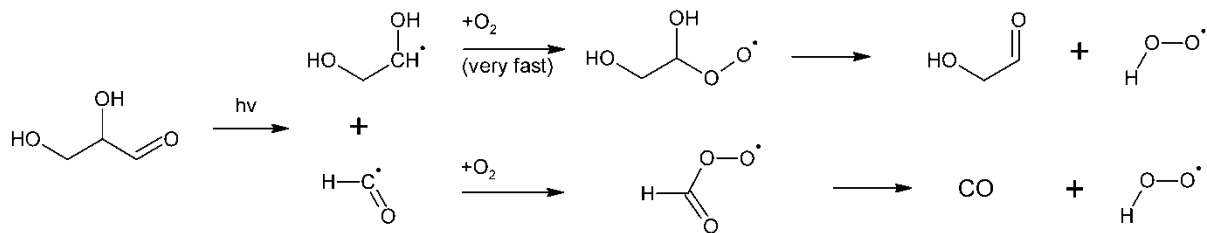
Table S5: Measured extinction coefficients of dihydroxyacetone (continued)

wavelength (nm)	Extinction (1/M/cm)	uncertainty in Extinction (1/M/cm)
368	0.02	0.01
370	0.00	0.00
372	0.01	0.01
374	0.00	0.00
376	0.00	0.00
378	0.00	0.00
380	0.00	0.00
382	0.01	0.01
384	0.00	0.01
386	0.00	0.00
388	0.00	0.00
390	0.00	0.00
392	0.00	0.00
394	0.00	0.00
396	0.00	0.00
398	0.00	0.00
400	0.00	0.00

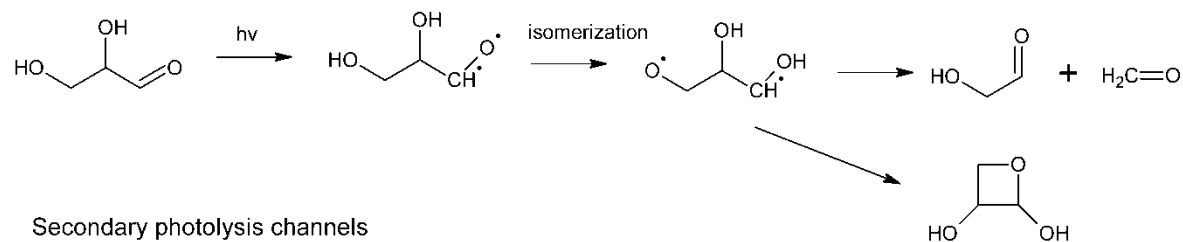
#### 14. Expected Chemical Mechanism of Glyceraldehyde Photolysis

Figure S28 illustrates all of the expected primary and secondary channels of glyceraldehyde photolysis. Note the presence of the glyceraldehyde structural isomer upon reaction between glycolaldehyde and formaldehyde. Significant production of this isomer could lead to underestimations in the photolysis quantum yield of glyceraldehyde with the ESI-MS method described above.

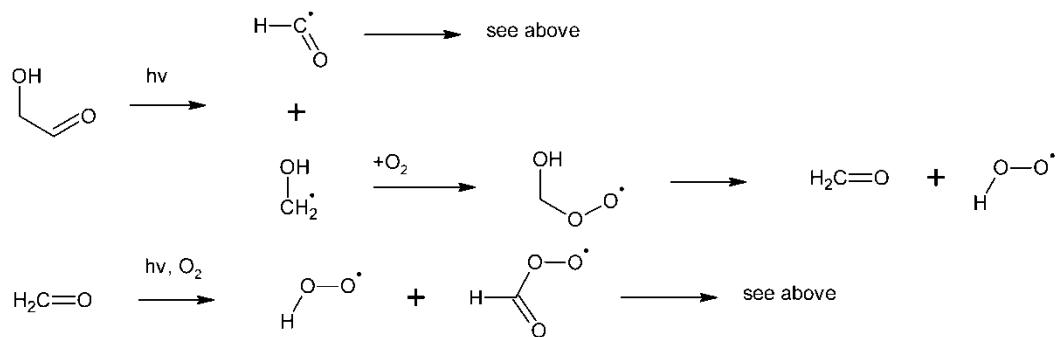
Expected Norrish-I channel



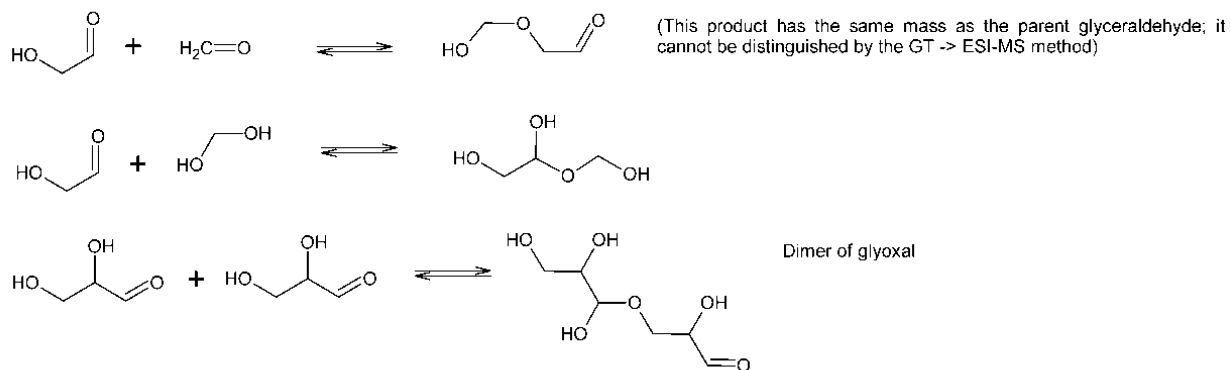
Expected Norrish-II channel



Secondary photolysis channels



Selected secondary processes complicating interpretation of data (not including hydration)



And other dimerization processes resulting in hemiacetals

Figure S28: Chemical Mechanism of Glycerol Photolysis

**15. Comparison of Aqueous Photolysis and Aqueous Oxidation by OH for 4-hydroxy-3-methyl-but-2-enal, 3,6-oxoheptanoic acid, ketolimonaldehyde, and ketonorlimonic acid**

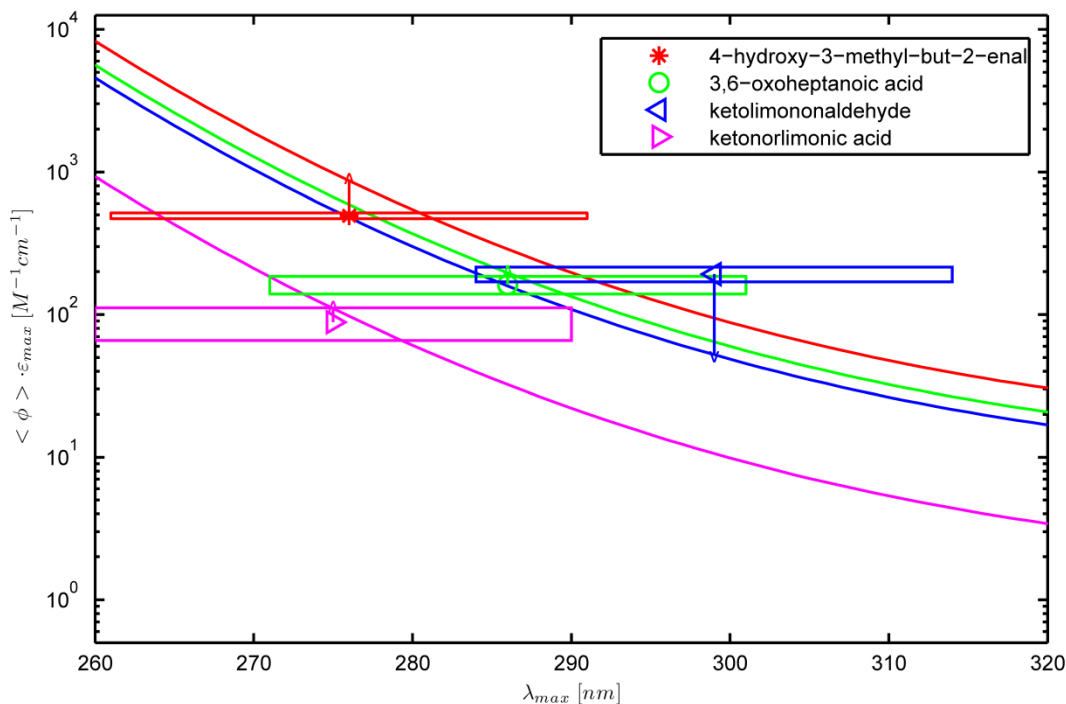


Figure S29: Comparison of aqueous photolysis at a solar zenith angle of  $20^\circ$  and aqueous oxidation by OH at a typical daytime concentration of  $10^{-13}$  M and a pH of 2. Molecules, denoted by the markers in the key, have arrows that point to their corresponding  $k_{OH}$ . Isoleths correspond to  $\lambda_{max}$  and  $\epsilon_{max} \cdot \langle \Phi \rangle$  values where  $Q = 1$  at the  $k_{OH}$  value of the molecule indicated with the same color. Rectangles indicate the bounds of the mean absolute errors calculated from TDDFT predictions of compounds with published extinction coefficients. Molecules with values of  $\lambda_{max}$  and  $\epsilon_{max} \cdot \langle \Phi \rangle$  that are below their corresponding  $k_{OH}$  value will be preferentially removed with oxidation by OH. Conversely, molecules with values of  $\lambda_{max}$  and  $\epsilon_{max} \cdot \langle \Phi \rangle$  that are above their corresponding  $k_{OH}$  value will be preferentially removed by aqueous photolysis.

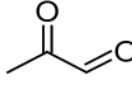
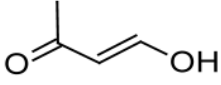
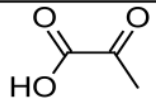
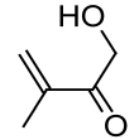
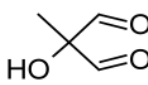
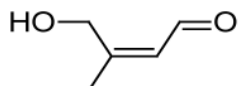
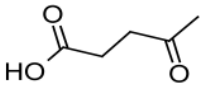
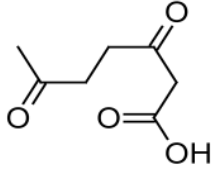
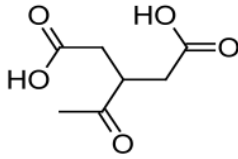
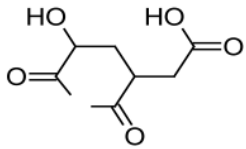
## 16. Parameters Used to Construct Figure 3

Table S6: Computational and experimental parameters used to model the SOA relevant compounds plotted in Figure 3.

Molecule Name	Molecule Ref.	KH (atm-m <sup>3</sup> /mol)	log(Khyd)	log(Khyd) 2nd most likely	KH Ref.	Khyd Ref.	kOH Aqueous pH = 2	kOH Aqueous pH = 6	kOH Aq. Ref.
methyl glyoxal	Fang (2012)	2.70E-07	1.82	-0.13	Betterton (1998)	SPARC	-	-	-
4-hydroxybut-3-en-2-one (keto-enol equilibrium forms 3-oxobutanal)	Fang (2012)	4.56E-08	1.53	0.71	HENRYWIN bond	SPARC	-	-	-
pyruvic acid	Fang (2012)	3.32E-09	-1.3	-	Khan (1992)	SPARC	-	-	-
1-hydroxy-3-methylbut-3-en-2-one	Fang (2012)	6.39E-06	-3.11	-	HENRYWIN bond	SPARC	-	-	-
2-methyl-2-oxidanyl-propanedial	Fang (2012)	1.29E-08	1.83	0.55	HENRYWIN bond	SPARC	-	-	-
4-hydroxy-3-methyl-but-2-enal	Fang (2012)	8.88E-10	-2.17	-	HENRYWIN group	SPARC	5.88E+09	5.88E+09	Buxton (1988) + SAR
levulinic acid	Jaoui (2006)	5.48E-11	-3.64	-	HENRYWIN group	SPARC	-	-	-
3,6-oxoheptanoic acid	Jaoui (2006)	3.29E-13	-1.28	-0.2	HENRYWIN group	SPARC	6.00E+08	4.00E+09	SAR
ketonorlimonic acid	Jaoui (2006)	1.17E-16	-5.34	-	HENRYWIN group	SPARC	2.10E+08	6.60E+08	SAR
ketolimaldehyde	Jaoui (2006)	4.55E-12	-1.09	-3.69	HENRYWIN group	SPARC	3.25E+09	3.25E+09	SAR

## 17. Structure of Molecules in Figure 3

Table S7: Molecular structures of SOA relevant compounds investigated in Figure 3

Label in Figure 3	Molecule Name	Molecule Reference	Structure
A	methyl glyoxal	Fang (2012)	
B	4-hydroxybut-3-en-2-one	Fang (2012)	
C	pyruvic acid	Fang (2012)	
D	1-hydroxy-3-methylbut-3-en-2-one	Fang (2012)	
E	2-methyl-2-oxidanyl-propanedial	Fang (2012)	
F	4-hydroxy-3-methyl-but-2-enal	Fang (2012)	
G	levulinic acid	Jaoui (2006)	
H	3,6-oxoheptanoic acid	Jaoui (2006)	
I	ketonorlimonic acid	Jaoui (2006)	
J	ketolimaldehyde	Jaoui (2006)	

## 18. Parameters Used to Construct Figures 4 and 5

Table S8: References and parameters used to generate Figures 4 and 5

Name	$\epsilon_{\max}$	$\lambda_{\max}$	Reference	aq. KOH pH = 2	aq. KOH pH = 6	Reference
ethanal	9	277	Xu (1993)	7.30E+08	7.30E+08	Buxton (1988)
acetone [2-propanone]	16.5	265.1	Xu (1993)	1.10E+08	1.10E+08	Buxton (1988)
2-pentanone	25.5	270.6	Xu (1993)	1.90E+09	1.90E+09	Buxton (1988)
methyl glyoxal [2-oxopropanal]	27.5	282.5	Mackinney (1948)	6.56E+08	6.56E+08	Lim (2005)
glyoxal [1,2-ethanedione]	5.8	267.5	Mackinney (1948)	1.05E+09	1.05E+09	Buxton (1988)
levulinic acid [4-oxopentanoic acid]	25.1	270	Mackinney (1948)	4.90E+08	6.00E+08	SAR
hydroxyacetone [1-hydroxy-2-propanone]	20	267	Steenken (1975)	5.11E+08	5.11E+08	SAR
dihydroxyacetone [1,3-Dihydroxy-2-propanone]	17.95	270	This Work	8.11E+08	8.11E+08	SAR
glyceraldehyde [2,3-dihydroxypropanal]	3.6	271	This Work	1.88E+09	1.88E+09	SAR
pyruvic acid [2-oxo-propanoic acid]	19.9	317.5	Mackinney (1948)	2.70E+08	7.00E+08	Ervens (2003)
methacrolein [2-methyl-2-propenal]	30	311	Liu (2009)	5.80E+09	5.80E+09	Liu (2009)
propanal	10.5	278	Xu (1993)	3.65E+09	3.65E+09	Monod (2005)
acrolein [2-propenal]	25	315	Sham (1995)	7.00E+09	7.00E+09	Buxton (1988)
butanal	14	284	Xu (1993)	3.77E+09	3.77E+09	Buxton (1988)
crotonaldehyde [2-butenal]	31.8	310	Mackinney (1948)	5.80E+09	5.80E+09	Buxton (1988)
2-butanone	20.5	267.6	Xu (1993)	9.00E+08	9.00E+08	Buxton (1988)
methylvinylketone [3-butene-2-one]	30	296	Renard (2013)	8.50E+09	8.50E+09	Buxton (1988)

## 19. Parameters Used to Construct Figures 2, 6, and S9-S13

**Table S9: Henry's Law constants used to construct Figures 2, 6, and S9-13**

Name	Functional Group	C#	kH (atm-m <sup>3</sup> /mol)	kH Ref.
formaldehyde	Aldehyde	1	3.37E-07	Betterton (1988)
ethanal (acetaldehyde)	Aldehyde	2	6.67E-05	Betterton (1988)
propanal	Aldehyde	3	7.34E-05	Betterton (1988)
butanal	Aldehyde	4	1.00E-04	Zhou (1990)
pentanal	Aldehyde	5	1.58E-04	Zhou (1990)
hexanal	Aldehyde	6	2.00E-04	Zhou (1990)
heptanal	Aldehyde	7	3.16E-04	Zhou (1990)
octanal	Aldehyde	8	5.01E-04	Zhou (1990)
nonanal	Aldehyde	9	1.00E-03	Zhou (1990)
decanal	Aldehyde	10	1.58E-03	Zhou (1990)
propan-2-one (acetone)	Ketone	3	3.16E-05	Staudingers (1996)
butan-2-one	Ketone	4	5.01E-05	Staudingers (1996)
pentan-2-one	Ketone	5	6.31E-05	Buttery (1971)
hexan-2-one	Ketone	6	1.58E-04	Buttery (1971)
heptan-2-one	Ketone	7	2.00E-04	Buttery (1971)
octan-2-one	Ketone	8	3.98E-04	Buttery (1971)
nonan-2-one	Ketone	9	6.31E-04	Buttery (1971)
ethanedial (glyoxal)	Dialdehyde	2	2.38E-09	Ip (2009)
propanedial	Dialdehyde	3	6.25E-08	HENRYWIN group estimate
butanedial	Dialdehyde	4	1.69E-08	HENRYWIN group estimate
pentanedial	Dialdehyde	5	2.39E-08	HENRYWIN group estimate
hexanedial	Dialdehyde	6	3.38E-08	HENRYWIN group estimate
heptanedial	Dialdehyde	7	4.77E-08	HENRYWIN group estimate

Table S9 (continued)

octanedial	Dialdehyde	8	6.74E-08	HENRYWIN group estimate
nonanedial	Dialdehyde	9	9.52E-08	HENRYWIN group estimate
decanedial	Dialdehyde	10	1.34E-07	HENRYWIN group estimate
undecanedial	Dialdehyde	11	1.90E-07	HENRYWIN group estimate
dodecanedial	Dialdehyde	12	2.68E-07	HENRYWIN group estimate
2-oxopropanal (methyl glyoxal)	Ketoaldehyde	3	2.70E-07	Betterton (1988)
3-oxobutanal	Ketoaldehyde	4	4.56E-08	HENRYWIN bond estimate
4-oxopentanal	Ketoaldehyde	5	1.12E-08	HENRYWIN group estimate
5-oxohexanal	Ketoaldehyde	6	1.58E-08	HENRYWIN group estimate
6-oxoheptanal	Ketoaldehyde	7	2.23E-08	HENRYWIN group estimate
7-oxooctanal	Ketoaldehyde	8	3.15E-08	HENRYWIN group estimate
8-oxononanal	Ketoaldehyde	9	4.45E-08	HENRYWIN group estimate
9-oxodecanal	Ketoaldehyde	10	6.29E-08	HENRYWIN group estimate
10-oxoundecanal	Ketoaldehyde	11	8.88E-08	HENRYWIN group estimate
butane-2,3-dione (biacetyl)	Diketone	4	1.33E-05	Betterton (1981)
pentane-2,4-dione	Diketone	5	2.35E-06	HENRYWIN experimental database
hexane-2,5-dione (acetonylacetone)	Diketone	6	7.39E-09	HENRYWIN group estimate
heptane-2,6-dione	Diketone	7	1.04E-08	HENRYWIN group estimate
octane-2,7-dione	Diketone	8	1.47E-08	HENRYWIN group estimate
nonane-2,8-dione	Diketone	9	2.08E-08	HENRYWIN group estimate
decane-2,9-dione	Diketone	10	2.94E-08	HENRYWIN group estimate
undecane-2,10-dione	Diketone	11	4.15E-08	HENRYWIN group estimate



Table S9 (continued)

dodecane-2,11-dione	Diketone	12	5.87E-08	HENRYWIN group estimate
tridecane-2,12-dione	Diketone	13	8.29E-08	HENRYWIN group estimate
1-hydroxypropan-2-one (hydroxyacetone)	Hydroxyketone	3	8.48E-09	HENRYWIN group estimate
4-hydroxybutan-2-one	Hydroxyketone	4	6.43E-10	HENRYWIN group estimate
5-hydroxypentan-2-one	Hydroxyketone	5	9.09E-10	HENRYWIN group estimate
6-hydroxyhexan-2-one	Hydroxyketone	6	1.28E-09	HENRYWIN group estimate
7-hydroxyheptan-2-one	Hydroxyketone	7	1.81E-09	HENRYWIN group estimate
8-hydroxyoctan-2-one	Hydroxyketone	8	2.56E-09	HENRYWIN group estimate
9-hydroxynonan-2-one	Hydroxyketone	9	3.62E-09	HENRYWIN group estimate
10-hydroxydecan-2-one	Hydroxyketone	10	5.11E-09	HENRYWIN group estimate
11-hydroxyundecan-2-one	Hydroxyketone	11	7.22E-09	HENRYWIN group estimate
12-hydroxydodecan-2-one	Hydroxyketone	12	1.02E-08	HENRYWIN group estimate
13-hydroxytridecan-2-one	Hydroxyketone	13	1.44E-08	HENRYWIN group estimate
14-hydroxytetradecan-2-one	Hydroxyketone	14	2.03E-08	HENRYWIN group estimate
2-oxoethanoic acid (glyoxylic acid)	Aldehydic Acid	2	9.17E-08	Ip (2009)
3-oxopropanoic acid	Aldehydic Acid	3	1.43E-10	Saxena and Hildeman (1996)
4-oxobutanoic acid	Aldehydic Acid	4	8.29E-11	HENRYWIN group estimate
5-oxopentanoic acid	Aldehydic Acid	5	1.17E-10	HENRYWIN group estimate
6-oxohexanoic acid	Aldehydic Acid	6	1.65E-10	HENRYWIN group estimate
7-oxoheptanoic acid	Aldehydic Acid	7	2.34E-10	HENRYWIN group estimate
8-oxooctanoic acid	Aldehydic Acid	8	3.30E-10	HENRYWIN group estimate
9-oxononanoic acid	Aldehydic Acid	9	4.66E-10	HENRYWIN group estimate
10-oxodecanoic acid	Aldehydic Acid	10	6.58E-10	HENRYWIN group estimate

Table S9 (continued)

11-oxoundecanoic acid	Aldehydic Acid	11	9.30E-10	HENRYWIN group estimate
2-hydroxyethanal (formic acid)	Hydroxyaldehyde	2	2.51E-08	Betterton (1988)
3-hydroxypropanal	Hydroxyaldehyde	3	9.74E-10	HENRYWIN group estimate
4-hydroxybutanal	Hydroxyaldehyde	4	1.38E-09	HENRYWIN group estimate
5-hydroxypentanal	Hydroxyaldehyde	5	1.94E-09	HENRYWIN group estimate
6-hydroxyhexanal	Hydroxyaldehyde	6	2.74E-09	HENRYWIN group estimate
7-hydroxyheptanal	Hydroxyaldehyde	7	3.88E-09	HENRYWIN group estimate
8-hydroxyoctanal	Hydroxyaldehyde	8	5.48E-09	HENRYWIN group estimate
9-hydroxynonanal	Hydroxyaldehyde	9	7.73E-09	HENRYWIN group estimate
10-hydroxydecanal	Hydroxyaldehyde	10	1.09E-08	HENRYWIN group estimate
11-hydroxyundecanal	Hydroxyaldehyde	11	1.54E-08	HENRYWIN group estimate
12-hydroxydodecanal	Hydroxyaldehyde	12	2.18E-08	HENRYWIN group estimate
13-hydroxytridecanal	Hydroxyaldehyde	13	3.08E-08	HENRYWIN group estimate
14-hydroxytetradecanal	Hydroxyaldehyde	14	4.35E-08	HENRYWIN group estimate
15-hydroxypentadecanal	Hydroxyaldehyde	15	6.14E-08	HENRYWIN group estimate
2-oxopropanoic acid (pyruvic acid)	Keto Acid	3	3.23E-09	Pocker (1969)
3-oxobutanoic acid (acetoacetic acid)	Keto Acid	4	3.69E-10	HENRYWIN bond estimate
4-oxopentanoic acid (levulinic acid)	Keto Acid	5	4.89E-10	HENRYWIN bond estimate
5-oxohexanoic acid	Keto Acid	6	6.49E-10	HENRYWIN bond estimate
6-oxoheptanoic acid	Keto Acid	7	8.62E-10	HENRYWIN bond estimate
7-oxooctanoic acid	Keto Acid	8	1.14E-09	HENRYWIN bond estimate
8-oxononanoic acid	Keto Acid	9	1.52E-09	HENRYWIN bond estimate
9-oxodecanoic acid	Keto Acid	10	2.02E-09	HENRYWIN bond estimate

Table S10: Hydration equilibrium constants and acid-dissociation constants used to construct Figures 2, 6, and S9-13

Name	log(Khyd)1 A	log(Khyd)1 B	log(Khyd)2 A	log(Khyd)2 B	Khyd Ref.	pKa	pKa Ref.
formaldehyde	3.30103				Doussin (2013)		
ethanal (acetaldehyde)	0.079181				Doussin (2013)		
propanal	-0.070581				Doussin (2013)		
butanal	-0.221849				Doussin (2013)		
pentanal	-0.259637				Sham and Joens (1995)		
hexanal	-0.31				Sham and Joens (1995)		
heptanal	-0.27				SPARC		
octanal	-0.28				SPARC		
nonanal	-0.28				SPARC		
decanal	-0.29				SPARC		
propan-2-one (acetone)	-2.69897				Bell (1966)		
butan-2-one	-2.17				SPARC		
pentan-2-one	-2.21				SPARC		
hexan-2-one	-2.24				SPARC		
heptan-2-one	-2.26				SPARC		
octan-2-one	-2.27				SPARC		
nonan-2-one	-2.28				SPARC		
ethanedial (glyoxal)	2.31597		4.30103		Doussin (2013)		
propanedial	1.48		1.34		SPARC		
butanedial	1.16		-0.67		SPARC		
pentanedial	1.17		0.11		SPARC		
hexanedial	0.9		0.02		SPARC		
heptanedial	-0.02		-0.42		SPARC		

Table S10 (continued)

octanedial	-0.07		-0.5		SPARC		
nonanedial	-0.09		-0.59		SPARC		
decanedial	-0.11		-0.68		SPARC		
undecanedial	-0.12		-0.76		SPARC		
dodecanedial	-0.19		-0.78		SPARC		
2-oxopropanal (methyl glyoxal)	3.30103	-0.18	-0.13	1.1	Doussin (2013) & SPARC		
3-oxobutanal	1.53	-0.47	-0.49	0.71	SPARC		
4-oxopentanal	1.09	-1.15	-2.85	-1.28	SPARC		
5-oxohexanal	0.95	-1.32	-2.05	-0.33	SPARC		
6-oxoheptanal	0.72	-1.51	-2.13	-0.44	SPARC		
7-oxooctanal	-0.02	-1.88	-2.37	-0.56768	quad fit from adjacent data		
8-oxononanal	-0.07	-1.92	-2.46	-0.65739	quad fit from adjacent data		
9-oxodecanal	-0.09	-1.93	-2.54	-0.74	SPARC		
10-oxoundecanal	-0.1	-2	-2.63	-0.76	SPARC		
butane-2,3-dione (biacetyl)	0.30103		-1.08		Doussin (2013)		
pentane-2,4-dione	-0.39		-0.6		SPARC		
hexane-2,5-dione (acetylacetone)	-1.35		-3.28		SPARC		
heptane-2,6-dione	-1.43		-2.34		SPARC		
octane-2,7-dione	-1.61		-2.43		SPARC		
nonane-2,8-dione	-1.89		-2.5		SPARC		
decane-2,9-dione	-1.92		-2.59		SPARC		
undecane-2,10-dione	-1.93		-2.69		SPARC		

Table S10 (continued)

dodecane-2,11-dione	-1.93		-2.78		SPARC		
tridecane-2,12-dione	-1.93		-2.88		SPARC		
1-hydroxypropan-2-one (hydroxyacetone)	-1.05				SPARC		
4-hydroxybutan-2-one	-0.79				SPARC		
5-hydroxypentan-2-one	-2.94				SPARC		
6-hydroxyhexan-2-one	-2.19				SPARC		
7-hydroxyheptan-2-one	-2.27				SPARC		
8-hydroxyoctan-2-one	-2.36				SPARC		
9-hydroxynonan-2-one	-2.43				SPARC		
10-hydroxydecan-2-one	-2.51				SPARC		
11-hydroxyundecan-2-one	-2.6				SPARC		
12-hydroxydodecan-2-one	-2.6				SPARC		
13-hydroxytridecan-2-one	-2.75				SPARC		
14-hydroxytetradecan-2-one	-2.77				SPARC		
2-oxoethanoic acid (glyoxylic acid)	3.041393				Tur'yan (1998)	3.32	Dawson (1959)
3-oxopropanoic acid	1.46				SPARC	4.63	SPARC
4-oxobutanoic acid	-1.66				SPARC	4.37	SPARC
5-oxopentanoic acid	-0.47				SPARC	4.51	SPARC
6-oxohexanoic acid	-0.54				SPARC	4.6	SPARC
7-oxoheptanoic acid	-0.48				SPARC	4.68	SPARC
8-oxooctanoic acid	-0.58				SPARC	4.72	SPARC
9-oxononanoic acid	-0.69				SPARC	4.73	SPARC
10-oxodecanoic acid	-0.79				SPARC	4.74	SPARC

Table S10 (continued)

11-oxoundecanoic acid	-0.89				SPARC	4.74	SPARC
2-hydroxyethanal (formic acid)	1.1959				Amyes (2007)	3.77	Brown (1955)
3-hydroxypropanal	1.36				SPARC		
4-hydroxybutanal	-1.16				SPARC		
5-hydroxypentanal	-0.23				SPARC		
6-hydroxyhexanal	-0.32				SPARC		
7-hydroxyheptanal	-0.41				SPARC		
8-hydroxyoctanal	-0.49				SPARC		
9-hydroxynonanal	-0.57				SPARC		
10-hydroxydecanal	-0.65				SPARC		
11-hydroxyundecanal	-0.67				SPARC		
12-hydroxydodecanal	-0.68				SPARC		
13-hydroxytridecanal	-0.7				SPARC		
14-hydroxytetradecanal	-0.71				SPARC		
15-hydroxypentadecanal	-0.73				SPARC		
2-oxopropanoic acid (pyruvic acid)	0.146128				Esposito (1999)	2.45	IUPAC (1979)
3-oxobutanoic acid (acetoacetic acid)	-0.69				SPARC	3.59	IUPAC (1979)
4-oxopentanoic acid (levulinic acid)	-3.64				SPARC	4.6	IUPAC (1979)
5-oxohexanoic acid	-2.48				SPARC	4.8	IUPAC (1979)
6-oxoheptanoic acid	-2.62				SPARC	4.6	SPARC
7-oxooctanoic acid	-2.49				SPARC	4.68	SPARC
8-oxononanoic acid	-2.59				SPARC	4.72	SPARC
9-oxodecanoic acid	-2.69				SPARC	4.73	SPARC

Table S11: Aqueous and gas-phase OH oxidation rate constants used to construct Figures 2, 6, and S9-13

Name	KOH Aq pH = 2 [M <sup>-1</sup> s <sup>-1</sup> ]	KOH Aq pH = 6 [M <sup>-1</sup> s <sup>-1</sup> ]	KOH Aq Ref.	KOH Gas [cm <sup>3</sup> / molec/s]	KOH Gas Ref.
formaldehyde	1.00E+09	1.00E+09	Buxton (1998)	8.50E-12	Atkinson (2006)
ethanal (acetaldehyde)	7.30E+08	7.30E+08	Buxton (1998)	1.50E-11	Atkinson (2006)
propanal	3.29E+09	3.29E+09	Monod (2005)	2.00E-11	Atkinson (2006)
butanal	3.77E+09	3.77E+09	(2005)	2.40E-11	(2006)
pentanal	3.90E+09	3.90E+09	Monod (2005)	2.48E-11	Albaladejo (2002)
hexanal	2.50E+09	2.50E+09	Jurgens (2007)	2.60E-11	Albaladejo (2002)
heptanal	6.53E+09	6.53E+09	SAR	2.96E-11	Albaladejo (2002)
octanal	7.68E+09	7.68E+09	SAR	3.17E-11	SAR
nonanal	8.83E+09	8.83E+09	SAR	3.60E-11	Bowman (2003)
decanal	9.99E+09	9.99E+09	SAR	3.45E-11	SAR
propan-2-one (acetone)	1.10E+08	1.10E+08	Buxton (1998)	1.80E-13	Atkinson (2006)
butan-2-one	9.00E+08	9.00E+08	Buxton (1998)	1.20E-12	Atkinson (2006)
pentan-2-one	1.90E+09	1.90E+09	Buxton (1998)	4.56E-12	Atkinson (2000)
hexan-2-one	2.93E+09	2.93E+09	SAR	6.37E-12	Jiminez (2005)
heptan-2-one	4.09E+09	4.09E+09	SAR	1.17E-11	Atkinson (2000)
octan-2-one	5.25E+09	5.25E+09	SAR	1.10E-11	Wallington 1987
nonan-2-one	6.40E+09	6.40E+09	SAR	1.10E-11	SAR
ethanedial (glyoxal)	1.05E+09	1.05E+09	Buxton (1997)	1.10E-11	Atkinson (2006)
propanedial	2.46E+09	2.46E+09	SAR	1.32E-10	SAR
butanedial	2.86E+09	2.86E+09	SAR	4.70E-11	SAR
pentanedial	3.93E+09	3.93E+09	SAR	2.52E-11	Rogers (1989)
hexanedial	5.08E+09	5.08E+09	SAR	5.22E-11	SAR
heptanedial	6.23E+09	6.23E+09	SAR	5.36E-11	SAR

Table S11 (continued)

octanedial	7.38E+09	7.38E+09	SAR	5.50E-11	SAR
nonanedial	8.53E+09	8.53E+09	SAR	5.64E-11	SAR
decanedial	1.00E+10	1.00E+10	SAR	5.79E-11	SAR
undecanedial	1.00E+10	1.00E+10	SAR	5.93E-11	SAR
dodecanedial	1.00E+10	1.00E+10	SAR	6.07E-11	SAR
2-oxopropanal (methyl glyoxal)	6.56E+08	6.56E+08	SAR	1.30E-11	SAR
3-oxobutanal	1.34E+09	1.34E+09	SAR	6.65E-11	SAR
4-oxopentanal	1.82E+09	1.82E+09	SAR	2.63E-11	SAR
5-oxohexanal	2.78E+09	2.78E+09	SAR	3.68E-11	SAR
6-oxoheptanal	3.92E+09	3.92E+09	SAR	3.15E-11	SAR
7-oxooctanal	5.07E+09	5.07E+09	SAR	3.30E-11	SAR
8-oxononanal	6.22E+09	6.22E+09	SAR	3.44E-11	SAR
9-oxodecanal	7.37E+09	7.37E+09	SAR	3.58E-11	SAR
10-oxoundecanal	8.52E+09	8.52E+09	SAR	3.72E-11	SAR
butane-2,3-dione (biacetyl)	1.86E+09	1.86E+09	Schaefer (2012)	2.48E-13	Dagaut (1988)
pentane-2,4-dione	9.90E+09	9.90E+09	Buxton (1998)	9.07E-11	Zhou (2008)
hexane-2,5-dione (acetylacetone)	6.10E+08	6.10E+08	Schaefer (2012)	5.67E-12	SAR
heptane-2,6-dione	1.41E+09	1.41E+09	SAR	1.61E-11	SAR
octane-2,7-dione	2.52E+09	2.52E+09	SAR	1.09E-11	SAR
nonane-2,8-dione	3.67E+09	3.67E+09	SAR	1.23E-11	SAR
decane-2,9-dione	4.82E+09	4.82E+09	SAR	1.37E-11	SAR
undecane-2,10-dione	5.97E+09	5.97E+09	SAR	1.51E-11	SAR



Table S11 (continued)

dodecane-2,11-dione	7.13E+09	7.13E+09	SAR	1.65E-11	SAR
tridecane-2,12-dione	8.28E+09	8.28E+09	SAR	1.80E-11	SAR
1-hydroxypropan-2-one (hydroxyacetone)	1.00E+09	1.00E+09	SAR	3.00E-12	Atkinson (2006)
4-hydroxybutan-2-one	2.59E+09	2.59E+09	Buxton (1998)	1.39E-11	SAR
5-hydroxypentan-2-one	3.62E+09	3.62E+09	SAR	9.64E-12	SAR
6-hydroxyhexan-2-one	4.77E+09	4.77E+09	SAR	1.11E-11	SAR
7-hydroxyheptan-2-one	5.92E+09	5.92E+09	SAR	1.25E-11	SAR
8-hydroxyoctan-2-one	7.07E+09	7.07E+09	SAR	1.39E-11	SAR
9-hydroxynonan-2-one	1.00E+10	1.00E+10	SAR	1.53E-11	SAR
10-hydroxydecan-2-one	1.00E+10	1.00E+10	SAR	1.67E-11	SAR
11-hydroxyundecan-2-one	1.00E+10	1.00E+10	SAR	1.81E-11	SAR
12-hydroxydodecan-2-one	1.00E+10	1.00E+10	SAR	1.95E-11	SAR
13-hydroxytridecan-2-one	1.00E+10	1.00E+10	SAR	2.09E-11	SAR
14-hydroxytetradecan-2- one	1.00E+10	1.00E+10	SAR	2.24E-11	SAR
2-oxoethanoic acid (glyoxylic acid)	4.70E+08	2.60E+09	Ervens (2003)	1.28E-11	SAR
3-oxopropanoic acid	9.73E+08	1.39E+09	SAR	6.64E-11	SAR
4-oxobutanoic acid	1.42E+09	1.66E+09	SAR	2.63E-11	SAR
5-oxopentanoic acid	2.20E+09	2.88E+09	SAR	3.68E-11	SAR
6-oxohexanoic acid	3.34E+09	4.03E+09	SAR	3.15E-11	SAR
7-oxoheptanoic acid	4.49E+09	5.18E+09	SAR	3.29E-11	SAR
8-oxooctanoic acid	5.64E+09	6.34E+09	SAR	3.44E-11	SAR
9-oxononanoic acid	6.79E+09	7.49E+09	SAR	3.58E-11	SAR
10-oxodecanoic acid	7.94E+09	8.64E+09	SAR	3.72E-11	SAR

Table S11 (continued)

11-oxoundecanoic acid	9.09E+09	9.79E+09	SAR	3.86E-11	SAR
2-hydroxyethanal (formic acid)	1.14E+09	1.14E+09	SAR	1.10E-11	Atkinson (2006)
3-hydroxypropanal	3.21E+09	3.21E+09	SAR	3.45E-11	SAR
4-hydroxybutanal	3.86E+09	3.86E+09	SAR	3.03E-11	SAR
5-hydroxypentanal	4.97E+09	4.97E+09	SAR	3.17E-11	SAR
6-hydroxyhexanal	6.12E+09	6.12E+09	SAR	3.31E-11	SAR
7-hydroxyheptanal	7.27E+09	7.27E+09	SAR	3.45E-11	SAR
8-hydroxyoctanal	8.43E+09	8.43E+09	SAR	3.59E-11	SAR
9-hydroxynonanal	9.58E+09	9.58E+09	SAR	3.74E-11	SAR
10-hydroxydecanal	1.00E+10	1.00E+10	SAR	3.88E-11	SAR
11-hydroxyundecanal	1.00E+10	1.00E+10	SAR	4.02E-11	SAR
12-hydroxydodecanal	1.00E+10	1.00E+10	SAR	4.16E-11	SAR
13-hydroxytridecanal	1.00E+10	1.00E+10	SAR	4.30E-11	SAR
14-hydroxytetradecanal	1.00E+10	1.00E+10	SAR	4.44E-11	SAR
15-hydroxypentadecanal	1.00E+10	1.00E+10	SAR	4.58E-11	SAR
2-oxopropanoic acid (pyruvic acid)	2.70E+08	7.00E+08	Ervens (2003)	6.52E-13	SAR
3-oxobutanoic acid (acetoacetic acid)	2.27E+08	2.73E+08	SAR	2.10E-12	SAR
4-oxopentanoic acid (levulinic acid)	4.94E+08	6.01E+08	SAR	1.18E-11	SAR
5-oxohexanoic acid	1.35E+09	1.48E+09	SAR	1.82E-11	SAR
6-oxoheptanoic acid	2.47E+09	2.60E+09	SAR	1.30E-11	SAR
7-oxooctanoic acid	3.62E+09	3.75E+09	SAR	1.44E-11	SAR
8-oxononanoic acid	4.78E+09	4.90E+09	SAR	1.58E-11	SAR
9-oxodecanoic acid	5.93E+09	6.05E+09	SAR	1.72E-11	SAR

## 20. References

- Albaladejo, J., Ballesteros, B., Jimenez, E., Martin, P., and Martinez, E.: A plp-lif kinetic study of the atmospheric reactivity of a series of C4-C7 saturated and unsaturated aliphatic aldehydes with OH, *Atmos. Environ.*, 36, 3231 - 3239, 2002.
- Amyes, T. L., and Richard, J. P.: Enzymatic catalysis of proton transfer at carbon: Activation of triosephosphate isomerase by phosphite dianion, *Biochemistry*, 46, 5841-5854, 10.1021/bi700409b, 2007.
- Atkinson, R., Tuazon, E. C., and Aschmann, S. M.: Atmospheric chemistry of 2-pentanone and 2-heptanone, *Environ. Sci. Technol.*, 34, 623-631, 10.1021/es9909374, 2000.
- Atkinson, R., Baulch, D. L., Cox, R. A., Crowley, J. N., Hampson, R. F., Hynes, R. G., Jenkin, M. E., Rossi, M. J., and Troe, J.: Evaluated kinetic and photochemical data for atmospheric chemistry: Volume II; gas phase reactions of organic species, *Atmos. Chem. Phys.*, 6, 3625-4055, 10.5194/acp-6-3625-2006, 2006.
- Beeby, A., Mohammed, D. b. H., and Sodeau, J. R.: Photochemistry and photophysics of glycolaldehyde in solution, *J. Am. Chem. Soc.*, 109, 857-861, 10.1021/ja00237a036, 1987.
- Betterton, E. A., and Hoffmann, M. R.: Henry's law constants of some environmentally important aldehydes, *Environ. Sci. Technol.*, 22, 1415-1418, 10.1021/es00177a004, 1988.
- Betterton, E. A.: The partitioning of ketones between the gas and aqueous phases, *Atmos. Environ.*, 25, 1473-1477, 1991.
- Bowman, J. H., Barket, D. J., and Shepson, P. B.: Atmospheric chemistry of nonanal, *Environ. Sci. Technol.*, 37, 2218 - 2225, 2003.
- Brown, H. C. e. a., in , Braude, E. A., and Nachod, F. C.: Determination of organic structures by physical methods, v. 1, Academic Press, 1955.
- Buttery, R. G., Bomben, J. L., Guadagni, D. G., and Ling, L. C.: Volatilities of organic flavor compounds in foods, *J. Agric. Food. Chem.*, 19, 1045-1048, 10.1021/jf60178a004, 1971.
- Buxton, G. V., Greenstock, C. L., Helman, W. P., and Ross, A. B.: Critical review of rate constants for reactions of hydrated electrons, hydrogen atoms and hydroxyl radicals in aqueous solution, *J. Phys. Chem. Ref. Data*, 17, 513-886, 1988.
- Buxton, G. V., Malone, N. T., and Salmon, G. A.: Oxidation of glyoxal initiated by OH in oxygenated aqueous solution, *J. Chem. Soc., Faraday Trans.*, 93, 2889-2891, 1997.
- Cohen, S. G., Ostberg, B. E., Sparrow, D. B., and Blout, E. R.: Light-induced polymerization of some monomers containing allyl and methacrylate groups, *J. Polym. Sci.*, 3, 264-282, 10.1002/pol.1948.120030212, 1948.

Dagaut, P., Wallington, T. J., Liu, R., and Kurylo, M. J.: A kinetics investigation of the gas-phase reactions of OH radicals with cyclic ketones and diones: Mechanistic insights, *J. Phys. Chem.*, 92, 1988.

Davis, L.: The structure of dihydroxyacetone in solution, *Bioorg. Chem.*, 2, 197-201, 1973.

Dawson, R. M. C., Elliott, D. C., and Elliott, W. H.: Data for biochemical research, Oxford University Press on Demand, 1989.

Doussin, J. F., and Monod, A.: Structure-activity relationship for the estimation of OH-oxidation rate constants of carbonyl compounds in the aqueous phase, *Atmos. Chem. Phys. Discuss.*, 13, 15949-15991, 10.5194/acpd-13-15949-2013, 2013.

EPA Henrywin v3.20, U.S. Environmental Protection Agency: 2011.

Ervens, B., Gligorovski, S., and Herrmann, H.: Temperature-dependent rate constants for hydroxyl radical reactions with organic compounds in aqueous solutions, *Phys. Chem. Chem. Phys.*, 5, 1811-1824, 2003.

Esposito, A., Lukas, A., Meany, J. E., and Pocker, Y.: The reversible enolization and hydration of pyruvate: Possible roles of keto, enol, and hydrated pyruvate in lactate dehydrogenase catalysis, *Can. J. Chem.*, 77, 1108-1117, 10.1139/v99-071, 1999.

Fang, W., Gong, L., Zhang, Q., Cao, M., Li, Y., and Sheng, L.: Measurements of secondary organic aerosol formed from OH-initiated photo-oxidation of isoprene using online photoionization aerosol mass spectrometry, *Environ. Sci. Technol.*, 46, 3898-3904, 10.1021/es204669d, 2012.

Garcia-Jiminez, F., Zuniga, O. C., Garcia, Y. C., Cardenas, J., and Cuevas, G.: Experimental and theoretical study of the products from the spontaneous dimerization of dl- and d-glyceraldehyde, *J. Brazil Chem. Soc.*, 16, 467-476, 2005.

Glushonok, G. K., Petryaev, E. P., Turetskaya, E. A., and Shadyro, O. I.: Equilibrium between the molecular forms of glycolaldehyde and of dl-glyceraldehyde in aqueous solutions, *Zh. Fiz. Khim.*, 60, 2960-2970, 1986.

Glushonok, G. K., Glushonok, T. G., Maslovskaya, L. A., and Shadyro, O. I.: A <sup>1</sup>H and <sup>13</sup>C NMR and UV study of the state of hydroxyacetone in aqueous solutions, *Russ. J. Gen. Chem.*, 73, 1027-1031, 10.1023/b:rugc.0000007604.91106.60, 2003.

Gubina, T. I., Pankratov, A. N., Labunskaya, V. I., and Rogacheva, S. M.: Self-oscillating reaction in the furan series, *Chem. Heterocycl. Compd.*, 40, 1396-1401, 10.1007/s10593-005-0051-5, 2004.

Hilal, S. H., Bornander, L. L., and Carreira, L. A.: Hydration equilibrium constants of aldehydes, ketones and quinoxalines, *QSAR Comb. Sci.*, 24, 631-638, 10.1002/qsar.200430913, 2005.

Ip, H. S. S., Huang, X. H. H., and Yu, J. Z.: Effective Henry's law constants of glyoxal, glyoxylic acid, and glycolic acid, *Geophys. Res. Lett.*, 36, L01802, 10.1029/2008gl036212, 2009.

IUPAC, Data, C. o. E., Serjeant, E. P., and Dempsey, B.: Ionisation constants of organic acids in aqueous solution, Pergamon Press, 1979.

Jaoui, M., Corse, E., Kleindienst, T. E., Offenber, J. H., Lewandowski, M., and Edney, E. O.: Analysis of secondary organic aerosol compounds from the photooxidation of d-limonene in the presence of NO<sub>x</sub> and their detection in ambient PM<sub>2.5</sub>, *Environ. Sci. Technol.*, 40, 3819-3828, 10.1021/es052566z, 2006.

Jürgens, M., Jacob, F., Ekici, P., Friess, A., and Parlar, H.: Determination of direct photolysis rate constants and OH radical reactivity of representative odour compounds in brewery broth using a continuous flow-stirred photoreactor, *Atmos. Environ.*, 41, 4571-4584, <http://dx.doi.org/10.1016/j.atmosenv.2007.03.053>, 2007.

Karickhoff, S. W., Carreira, L. A., and Hilal, S. H. Sparc performs automated reasoning in chemistry v4.6, 2011.

Khan, I., and Brimblecombe, P.: Henry's law constants of low molecular weight organic acids, *J. Aerosol Sci*, 23, Supplement 1, 897-900, [http://dx.doi.org/10.1016/0021-8502\(92\)90556-B](http://dx.doi.org/10.1016/0021-8502(92)90556-B), 1992.

Liu, Y., El Haddad, I., Scarfogliero, M., Nieto-Gligorovski, L., Temime-Roussel, B., Quivet, E., Marchand, N., Picquet-Varrault, B., and Monod, A.: In-cloud processes of methacrolein under simulated conditions – part 1: Aqueous phase photooxidation, *Atmos. Chem. Phys.*, 9, 5093-5105, 10.5194/acp-9-5093-2009, 2009.

Mackinney, G., and Temmer, O.: The deterioration of dried fruit. IV. Spectrophotometric and polarographic studies, *J. Am. Chem. Soc.*, 70, 3586-3590, 10.1021/ja01191a013, 1948.

Malik, M., and Joens, J. A.: Temperature dependent near-UV molar absorptivities of glyoxal and gluteraldehyde in aqueous solution, *Spectrochim. Acta, Part A*, 56, 2653-2658, 2000.

Maroni: *Annales de Chimie*, 13, 757-787, 1957.

Martinez, A. M., Cushmac, G. E., and Rocek, J.: Chromic acid oxidation of cyclopropanols, *J. Am. Chem. Soc.*, 97, 6502-6510, 10.1021/ja00855a036, 1975.

Monod, A., Poulain, L., Grubert, S., Voisin, D., and Wortham, H.: Kinetics of OH-initiated oxidation of oxygenated organic compounds in the aqueous phase: New rate constants, structure activity relationships and atmospheric implications, *Atmos. Environ.*, 39, 7667-7688, 2005.

Monod, A., and Doussin, J. F.: Structure-activity relationship for the estimation of OH-oxidation rate constants of aliphatic organic compounds in the aqueous phase: Alkanes, alcohols, organic acids and bases, *Atmos. Environ.*, 42, 7611-7622, 2008.

Pocker, Y., Meany, J. E., Nist, B. J., and Zadorojny, C.: Reversible hydration of pyruvic acid. I. Equilibrium studies, *J. Phys. Chem.*, 73, 2879-2882, 10.1021/j100843a015, 1969.

Renard, P., Siekmann, F., Gandolfo, A., Socorro, J., Salque, G., Ravier, S., Quivet, E., Clément, J. L., Traikia, M., Delort, A. M., Voisin, D., Thissen, R., and Monod, A.: Radical mechanisms of methyl vinyl ketone oligomerization through aqueous phase OH-oxidation: On the paradoxical role of dissolved molecular oxygen, *Atmos. Chem. Phys. Discuss.*, 13, 2913-2954, 10.5194/acpd-13-2913-2013, 2013.

Rice, F. O.: The effect of solvent on the ultra violet absorption spectrum of a pure substance, *J. Am. Chem. Soc.*, 42, 727-735, 10.1021/ja01449a009, 1920.

Rogers, J. D.: Rate constant measurements for the reaction of the hydroxyl radical with cyclohexene, cyclopentene, and glutaraldehyde, *Environ. Sci. Technol.*, 23, 177 - 181, 1989.

Saxena, P., and Hildemann, L. M.: Water-soluble organics in atmospheric particles: A critical review of the literature and application of thermodynamics to identify candidate compounds, *J. Atmos. Chem.*, 24, 57-109, 1996.

Schaefer, T., Schindelka, J., Hoffmann, D., and Herrmann, H.: Laboratory kinetic and mechanistic studies on the OH-initiated oxidation of acetone in aqueous solution, *J. Phys. Chem. A*, 116, 6317-6326, 10.1021/jp2120753, 2012.

Schutze, M., and Herrmann, H.: Uptake of acetone, 2-butanone, 2,3-butanedione and 2-oxopropanal on a water surface, *Phys. Chem. Chem. Phys.*, 6, 965-971, 2004.

Sham, Y. Y., and Joens, J. A.: Temperature dependent near UV molar absorptivities of several small aldehydes in aqueous solution, *Spectrochim. Acta A*, 51, 247-251, 1995.

Staffelbach, T. A., Orlando, J. J., Tyndall, G. S., and Calvert, J. G.: The UV-visible absorption spectrum and photolysis quantum yields of methylglyoxal, *J. Geophys. Res.: Atmospheres*, 100, 14189-14198, 10.1029/95JD00541, 1995.

Staudinger, J., and Roberts, P. V.: A critical review of Henry's law constants for environmental applications, *Critical Reviews in Environmental Science and Technology*, 26, 205-297, 10.1080/10643389609388492, 1996.

Steenken, S., Jaenicke-Zauner, W., and Schulte-Frohlinde, D.: Photofragmentation of hydroxyacetone, 1,3-dihydroxyacetone, and 1,3-dicarboxyacetone in aqueous solution. An EPR study, *Photochem. Photobiol.*, 21, 21-26, 10.1111/j.1751-1097.1975.tb06624.x, 1975.

Tur'yan, Y. I.: Kinetics and equilibrium of the dehydration-hydration and recombination dissociation reactions of glyoxylic acid investigated by electrochemical methods, *Croat. Chem. Acta.*, 71, 727-743, 1998.

Wallington, T. J., and Kurylo, M. J.: Flash photolysis resonance fluorescence investigation of the gas-phase reactions of OH radicals with a series of aliphatic ketones over the temperature range 240-440 K, *J. Phys. Chem.*, 91, 1987.

Xu, H., Wentworth, P. J., Howell, N. W., and Joens, J. A.: Temperature dependent near-uv molar absorptivities of aliphatic aldehydes and ketones in aqueous solution, *Spectrochim. Acta A*, 49, 1171-1178, 1993.

Zhou, S. M., Barnes, I., Zhu, T., Bejan, I., Albu, M., and Benter, T.: Atmospheric chemistry of acetylacetone, *Environ. Sci. Technol.*, 42, 7905 - 7910, 2008.

Zhou, X., and Mopper, K.: Apparent partition coefficients of 15 carbonyl compounds between air and seawater and between air and freshwater; implications for air-sea exchange, *Environ. Sci. Technol.*, 24, 1864-1869, 10.1021/es00082a013, 1990.